X-615-66-92

NASA TM X- 55464

LOW ENERGY ELECTRONS MEASURED ON IMP II

BY

G. P. SERBU

E. J. R. MAIER

JANUARY 1966

NASA

GODDARD SPACE FLIGHT CENTER

GREENBELT, MARYLAND

X-615-66-92

LOW ENERGY ELECTRONS MEASURED ON IMP II

by
G. P. Serbu
and
E. J. R. Maier

Laboratory for Space Sciences

January 1966

GODDARD SPACE FLIGHT CENTER
Greenbelt, Maryland

ABSTRACT

The integral spectrum for low energy electrons has been measured with detailed definition of temperature and number density throughout the IMP II orbit. Electrons are found to have a Maxwellian distribution at energies below 2.0 eV with a component of higher energy. The electron temperature typically increases from above the ionosphere as the square of the radial distance, whereas the number density decreases approximately as the inverse cube of the distance out to 5 earth radii. From 5 earth radii to 15.9 R_e (apogee) the temperature remains between 1.0 and 2.0 eV and the number density remains between 25 and 50 electrons/cm^{-3}. The location of the magnetopause is not evident in the low energy electrons; however, a small temperature increase is noted at the shock boundary. An intensity increase is noted in the energetic electron component in the magnetosheath. Data for a six month period covering a 180° sector of the earth's environment is reported on.

CONTENTS

LIST OF ILLUSTRATIONS

LOW ENERGY ELECTRONS MEASURED ON IMP II

G. P. Serbu
and
E. J. R. Maier

I. INTRODUCTION

The Interplanetary Monitoring Platform, IMP II, or Explorer XXI, was launched from the Atlantic Missile Range, Cape Kennedy, Florida on 4 October 1964 at 03:52 Universal Time. On board both this spacecraft and IMP I were essentially identical retarding potential analyzer experiments. The following table presents the most significant initial orbital characteristics of the two missions.

IMP Launch	Orbital Period (Hours)	Inclination	Eccentricity	Apogee (km)	Perigee (km)	Spin (RPM)	Spin Axis Sun Angle
02:30 UT 11/27/63	93.5	33.33°	0.937	197616	192	22.3	111°
03:52 UT 10/4/64	34.67	33.53°	0.878	95016	200	14.2	131°

From the data in the table it is clear that while IMP II does not penetrate into the solar wind region to the extent IMP I has done, the IMP II mapping of the magnetosphere is more detailed than that of IMP I.

It is the purpose of this paper to present and discuss some of the results of the Retarding Potential Analyzer experiment on board the IMP II spacecraft. The primary objective of this experiment was to measure the electron and ion densities and energies as a function of orbital position. The integral spectrum of charged particle energies was obtained in two separate ranges: (1) a high resolution thermal range from 0 to 15 volts and (2) a low resolution range from 0 to 45 volts. Thus far, the electron current voltage characteristics have been analyzed for a period of 150 days in orbit; some preliminary results of this analysis are presented at this time. Future publications concerning this IMP II experiment will treat the ion data results obtained in this same time interval.

This paper considers the experimental arrangement including the geometric properties of the sensor, the procedure for data acquisition and analysis, and a discussion of some experimental results.

The observations of electron density distribution and electron temperature profiles obtained within the magnetosphere are presented. The locations of the magnetopause and shock front as determined from our data are given for sun-earth-satellite angles from 11° to 90°. A few observations made in the solar wind region are also presented and in addition measured values of satellite-to-plasma potentials are given.

II. EXPERIMENTAL ARRANGEMENT

The sensor, shown schematically in Figure 1, is a Faraday cup of planar geometry so designed as to measure the integral spectrum in the thermal range of energies for both ions and electrons.

The ambient plasma can be considered as incident on the spacecraft at the sensor at the vector sum of the plasma streaming velocity and the spacecraft velocity. The spacecraft velocity is at all times small compared to the velocity of even at 0.1 eV (1170°K) electron and thus can be ignored in the analysis of the electron data. When the spacecraft is near perigee, its velocity is comparable to ion velocities and it is necessary to include spacecraft attitude and velocity in the reduction of the ion data. The aperture is a hole of 5 cm^2 area over which is stretched a fine wire mesh having an optical transparency of 95 percent. Surrounding the aperture is a tungsten surface of 35 cm^2 area which is electrically connected to the aperture grid.

The accompanying table in Figure 1 shows the series of voltages which are programmed on the various trap elements in order to define the six modes of operation. For example, the electron spectrum is obtained as follows: a +45 volt aperture potential will effectively separate out from the entering plasma those ions with energies below 45 electron volts. The negative voltage programmed on the retarding grid sequentially and in synchronism with the telemetry system then yields the integral spectrum of electron current as a function of retarding potential in the interval from +5 to -45 volts. The suppressor grid is used to suppress secondary electrons emitted from the collector. In the electron mode the collector is maintained positive in order to insure collection of all electrons which pass through the retarding and suppressor grids. The retarding potential is programmed in fifteen discrete voltage increments from +5 to -45 volts in a period of 5.2 seconds. The entire ion, electron and net current measurement cycle is completed every 648 seconds.

Examination of the potential on the suppressor illustrates that during the two electron modes of operation and during the low resolution ion mode the photoemission currents from the collector have been suppressed; however,

IMP II - EXPLORER XXI

RETARDING POTENTIAL ANALYSER

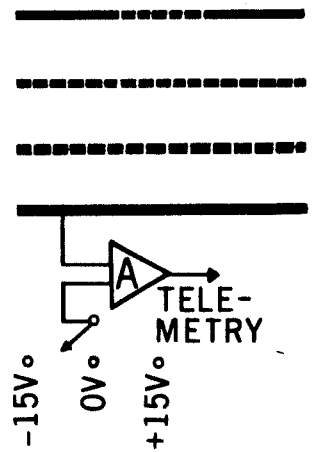

APERTURE	ELECTRON		ION		NET CURRENT	
	+50	+15	-50	-15	0	0
RETARDING	-45→0→+5	-15→0→+0.5	-5→0→+45	-0.5→0→+15	0	0
SUPPRESSOR	0	0	-50	-15	0	0
COLLECTOR	+15	+15	-15	-15	0	0
ELECTROMETER POLARITY	-	-	+	+	-	+

Figure 1. Schematic representation of the sensor and the experiment voltage program.

photoelectrons emitted from the suppressor grid itself will reach the collector and register as a negative current component which varies as a function of the solar aspect. The magnitude of this current being directly proportional to the area of the grid wires is expected to be of the order of 10^{-9} amperes. In the analysis of the electron current use is made of the spacecraft optical aspect sensor to compute the precise times at which the sun vector lies in the plane defined by the spin axis and the sensor normal. Data obtained during the time when the sun is within ±70 degrees of the trap normal are eliminated from the analysis. In practice this means that five data points are eliminated from the total spectrum of 15 data points. Due to the fact that the satellite spin rate is not synchronous with the retardation program the data points which are dropped in the analysis fortunately do not always fall in that portion of the spectrum which is changing rapidly. The net effect is that not all current voltage characteristics obtained can subsequently be analyzed to yield electron temperatures and densities. However, the large amounts of data received still allow us to make a meaningful measurement at increments of 0.1 earth radius along nearly the entire orbit, the exception being at altitudes below 10,000 kilometers where the satellite velocity and orientation are changing much too rapidly in the time interval of 5.2 seconds required to obtain one spectrum.

The collector current is measured by an electrometer whose sensitivity ranges from 1×10^{-11} amperes to 1×10^{-7} amperes full scale. The analog output of the electrometer is presented to the telemetry system as a voltage from 0 to 5 volts full scale. During the electron mode of operation the electrometer can respond only to negative currents, and during the ion mode the response is to positive currents.

Incorporated within the experiment is an internal calibration capability. One step in the data analysis procedure is to check this internal calibration and make appropriate corrections. For the first three months in orbit, the electrometer gain change was less than 5 percent. During January and February 1965 the satellite operation was intermittent due to an unfavorable sun-solar paddle aspect angle which gradually improved so that by March full time operation was again achieved. There were no significant gain changes in the electronics during this period.

III. DATA AND ANALYSIS

Figure 2 is a sample of the current voltage characteristics obtained with the Retarding Potential Analyzer experiment as flown on IMP II. Plotted on a logarithmic scale is the negative current as measured by the electrometer as a function of the linear abscissa which is the retarding potential in volts. Two

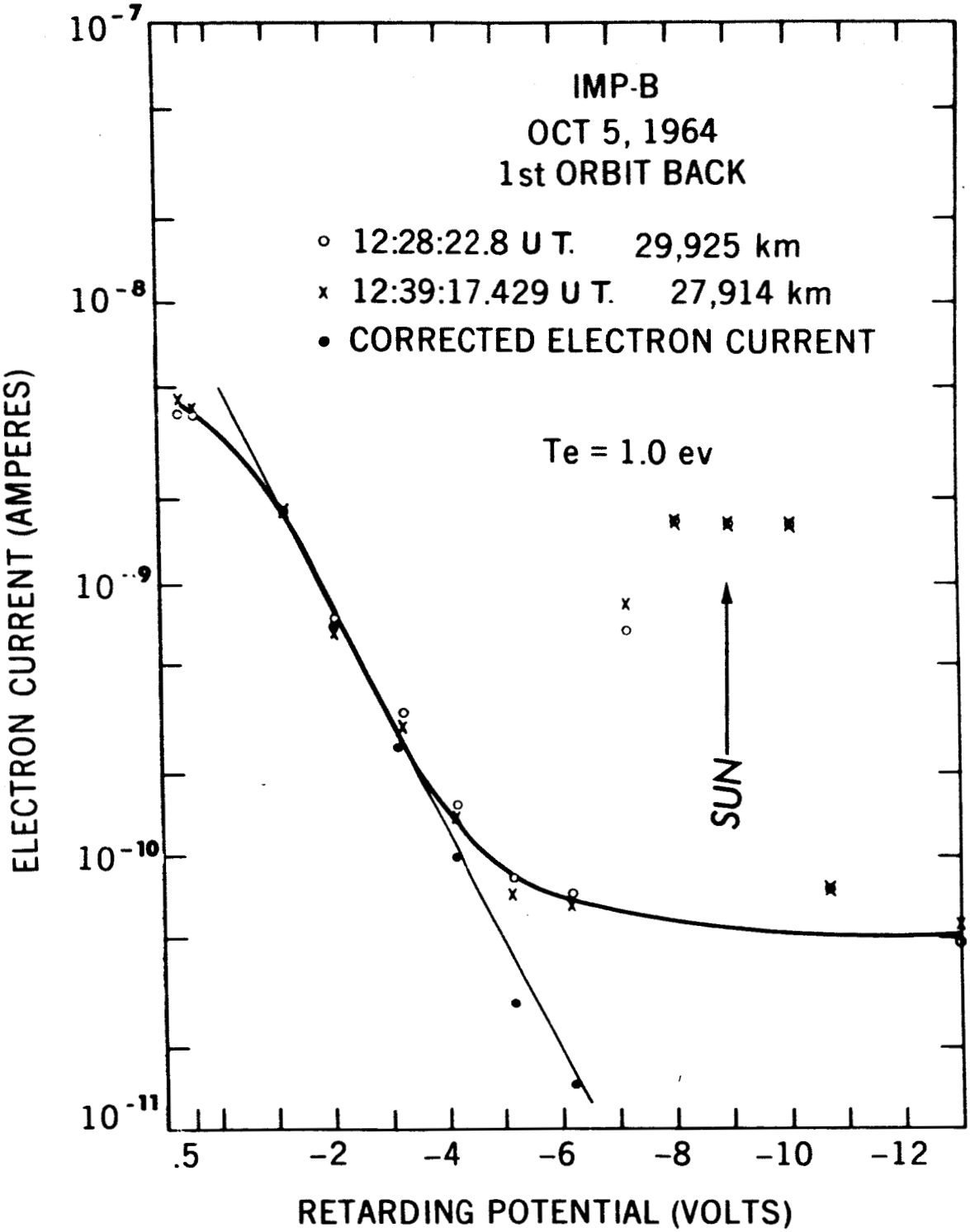

Figure 2. Sample electron current-voltage retardation curves. The logarithmic negative current is plotted as a function of the linear retardation potential in volts.

spectrums obtained within 11 minutes of each other on 5 October 1964 are illustrated as the open circles and crosses in Figure 2. In the elapsed time of 11 minutes the satellite has moved 2011 km at an altitude of approximately 28,000 km; however, the two spectrums are virtually identical in shape and form. Each spectrum is obtained within 5.2 seconds which corresponds to 15 km translational motion, thus illustrating that in this region of the earth's magnetosphere the plasma characteristics are not changing too rapidly. The arrow in the figure marks the precise point during the spectrum at which the sun vector is normal to the trap, thus indicating that the five data points symmetric in time about the sun position contain photoemission currents and that these points should be discarded in the analysis. A smooth curve as shown can be drawn through the remaining 10 data points.

It has been found that the data can be well fitted by considering the plasma to consist of two components having Maxwellian energy distribution. It should be pointed out that both components are omnidirectional. One, the "thermal component," has a mean energy below 4 electron volts; the second, the so-called "high energy component" has a mean energy much higher than 4 electron volts. Separation of the two components results in the retardation spectrum for the "thermal component" as illustrated by the solid dot curve in Figure 2. The one hundred-to-one logarithmic decrease in electron current with increasing retarding voltage establishes that the energy distribution of the thermal component is Maxwellian. Note that the high energy tail is only partially retarded due to the limited range of the sweep voltage in the experiment. This limited retardation does not enable us to distinguish the true nature of the energy distribution of the "high energy" component; this is, an equally good fit to the data would be obtained using other functional relationships. The exponential is used primarily for convenience; its use in the case of the high energy component does not necessarily imply the existence of thermal equilibrium for that component.

A computer program has been generated in order to process the satellite telemetry information, convert this to current (I) - voltage (V) characteristics and eliminate the data points which contain a photocurrent component. Analysis of the selected, corrected data points is then carried out by the computer. The analysis consists of performing a least squares fit by an iterative process to an appropriate combination of exponential distributions, using only the data obtained in the retarding region of the basic I-V curve. The data fit to the computed exponential has typically a fractional root mean deviation in the range from 0.001 to 0.1. The temperatures of the two distributions are then directly obtained as the exponent coefficients of the best fitted exponentials. The density is computed from the value of the thermal current at the satellite potential and the temperature of the "thermal component." In this case the satellite potential is taken to be the negative value of the sweep voltage at the inflection of the curve.

At times, should the satellite be more negative than 0.5 volts, no inflection is obtained and thus, density values cannot be computed. In general, the satellite potential is positive between 0 and +2 volts with respect to the plasma for all parts of the orbit at distances greater than about 2 earth radii.

In most cases the analysis program has worked very well; the only difficulty experienced with this procedure has been for data obtained in the transition region (beyond $10R_e$) where the ratio of the maximum thermal electron current values to the mean of the high energy component value is less than three to one, thus making it somewhat difficult to meaningfully separate the two individual components.

Throughout much of the spacecraft orbit, the Debye length, and thus the "sheath thickness," is in excess of 10 cm. The proper interpretation of the probe characteristic in the unretarded portion of the sweep is extremely complex. Theoretical studies (Parker, 1965) assuming idealized, but reasonable, boundary conditions indicate that the enhancement of the effective area over the geometric area may be of the order of a factor 5 to 10. The factor of ten enhancement is predicted if the field in the vicinity of the trap is defined by Laplace's equation. This is evidently an upper limit for the enhancement. The presence of a sheath will screen the local field and yield a smaller enhancement factor.

Results obtained by programming different potentials on the entrance aperture do not indicate as severe an increase of observed saturation current with applied accelerating potential as is predicted for the idealized geometry. The observation of a nonlinear dependence on accelerating potential is evidence of the above-mentioned screening. Thus the minimum possible effective area is the geometric area of the aperture, A_G. The maximum possible effective area is that predicted for zero local charge density; its value is $10A_G$. Applying these two possible values for the area to our observed saturation electron currents yields upper and lower bounds for the electron density. By combining Parker's predicted enhancement factor and the observed effect of different acceleration potentials, we arrive at 4 as the best value for the enhancement. The densities presented are obtained by using $4A_G$ as the effective area. From the above considerations it is believed that this augmentation factor is known to within a factor of 2 so that the absolute values of densities may be in error by a factor of 2. It should be emphasized that relative errors are determined by the stability of the electronics, which is of the order of 5%.

IV. RESULTS

1. Magnetosphere

Figure 3 is a view of the latitudinal excursion of the IMP II spacecraft. The satellite passes through the earth's equatorial plane from North to South on the outbound leg of the trajectory. In general at large distances the satellite is in the southern hemisphere and within 30° of the geographic equator. Closer in than 5 earth radii on the inbound trajectory the satellite crosses through the equatorial plane toward its maximum northern latitude of 33.5°. Essentially, then, within the magnetosphere the IMP II orbit is near the equatorial plane and it is useful to compare the data with the Whistler profiles which are taken in the equatorial plane.

Carpenter and Smith [1964] have presented experimental results from Whistler observations which indicate that in the equatorial plane the electron distribution can be represented in accordance with $N_e \propto R_e^{-3}$ or $N_e \propto R_e^{-4}$, where the electron density N_e is a smooth function of the geocentric distance R_e in earth radii. This relationship exists out to about 5 earth radii.

The knee Whistlers described by Carpenter and Smith [1964] and Carpenter [1963], [1965] present a second type of measured electron distribution in which the density suddenly drops a factor of 50 or more at distances varying between 3 and 5 earth radii. The knee in the equatorial profile leads them to classify the magnetosphere into two regions: an inner relatively quiet magnetosphere in which particles are in some form of a modified diffusive equilibrium, and an outer region having extremely low densities of thermal plasma.

Figure 4 is a plot of the electron density as a function of geocentric distance along the orbit. Included in this plot are data from IMP I taken on 27 October 1963 (Serbu, 1964, open box points) and data from two orbits of IMP II taken on the inbound pass on 8 October 1964 and the outbound pass of 17 October 1964. In the region from $2R_e$ to $5R_e$ the density falls off as the -3.4 power of the distance; from 5 to $10R_e$ the density is observed to be in the range from 25 to 80 el/cm^3. This observation of approximately uniform density from about 5 to $10R_e$ has been repeated consistently and we will subsequently discuss it in detail. It is of interest to note that the IMP I and IMP II density results have the same general rate of decay with distance; however, the 1963 data seem lower by about a factor of 3. Since the two satellites were in essentially the same region of space, we attribute this difference in measured density value to a temporal variation. Also shown in Figure 4 are four values of electron density at 1000 km, which were computed from topside ionograms obtained by the Alouette I satellite near the time of the IMP II data observations. Three out of four of the ionogram

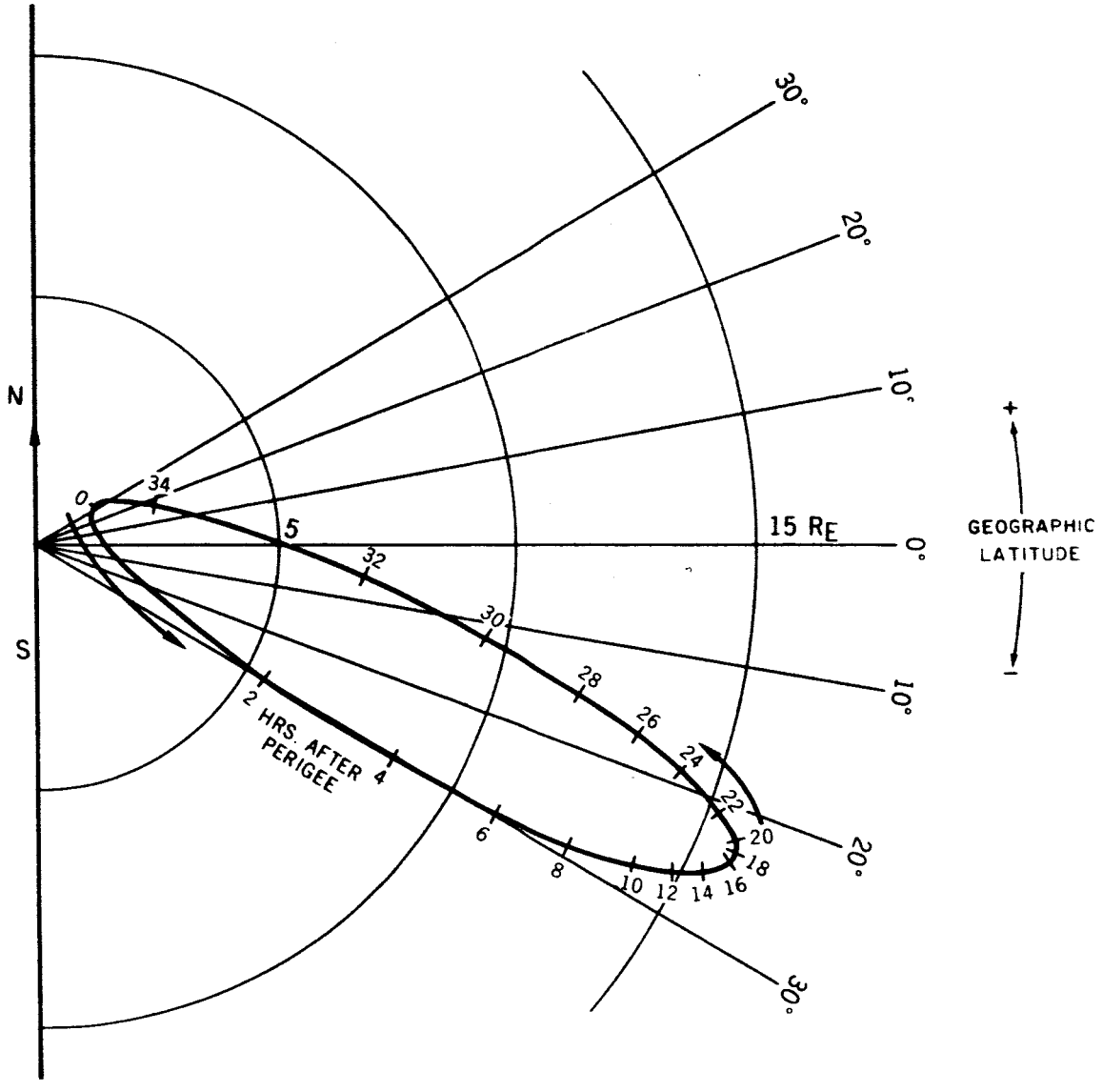

Figure 3. A view of the latitudinal excursion of the IMP II spacecraft. IMP II was launched with the line of apsides extending toward the sun, but inclined about -20° to the ecliptic.

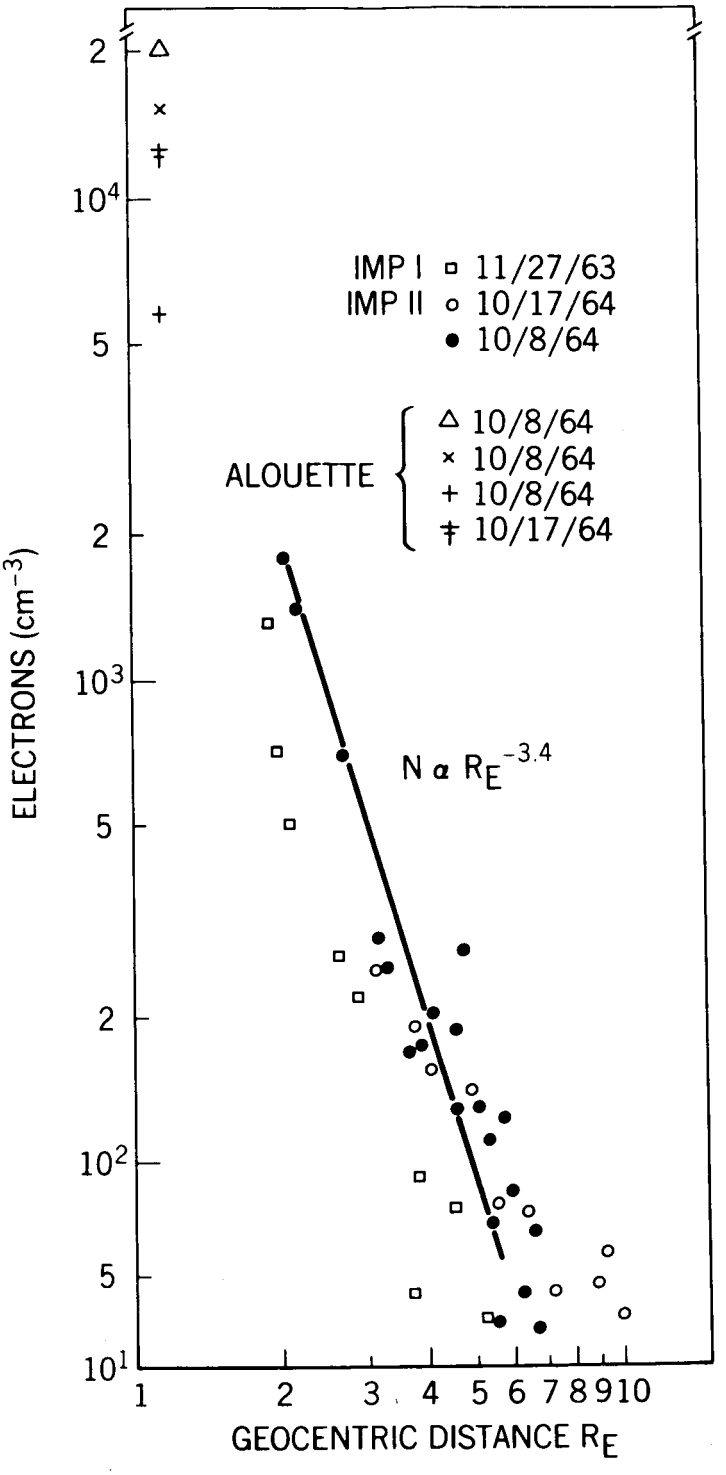

Figure 4. Plot of the electron density as a function of geocentric distance. Data obtained from IMP I and IMP II and the topside sounder satellite, Alouette I are presented.

values compare favorably with extrapolated IMP measurements. Additional comparisons with Alouette are made in Figures 8 through 14. The purpose is to illustrate that the extrapolated IMP measurement, in general, agrees within a factor of 3 with the Alouette value at 1000 km.

The 11 October 1964 data, Figure 5, illustrates more clearly the shape of an individual profile. Data points closer in than 2 earth radii are difficult to obtain due to poor telemetry acquisition and also due to the fact that the orbital velocity is sufficiently high to cause significant spacecraft motion during the time of one sweep. As can be seen neither of the density profiles in Figures 4 and 5 indicate a knee-type of fall-off in the region from 3 to $5R_e$; in fact, our density at $5R_e$ is just about a factor of 10 above that reported by Angerami and Carpenter, [1965] and by Taylor, et al., [1965]. Obayashi [1965] has used the differential Doppler shift of the harmonically related transmitters (40 and 360 Mc/s) on OGO-A to determine the local electron density at the spacecraft. He obtains an average local density at local noon 16 November 1964 of 1 to 2×10^3 cm^{-3} at a geocentric distance of $3.2R_e$. The IMP II satellite was at $3.3R_e$ on 16 November 1964 at 11:03 UT; the density value as measured by us was 1.04×10^3 electrons cm^{-3}. Note also the electron density profile displayed in Figure 14. These data were obtained about 44 hours after Obayashi's measurement, and agree very well with his result.

Slish [1965] has recently reported the results of an antenna impedance measurement associated with cosmic noise observations by an experiment on the spacecraft Zond II launched November 1964. Two independent observations are presented. A peak attributed to electron plasma resonance is observed in the 210 kc receiver response at $4R_e$ geocentric. This observation yields a local density of 550 electrons cm^{-3}. The second observation is an analysis of the receiver response to a signal above the plasma frequency in terms of the effect of the local plasma density on the radiation resistance of the antenna. Interpreted in this manner, a radial dependence $n_e = 1.3 \times 10^5 (R/R_o)^{-4}$ valid from 4 to $7R_e$ is obtained. Both the general radial dependence and the specific value of 100 electrons cm^{-3} at 6 earth radii are in excellent agreement with our result.

In the region of space through which we have noted a smooth fall-off rate in the density of electrons we also observe that the temperature of the low energy electrons is increasing according to a power law of the geocentric distance. The 27 November 1963 IMP I temperature profile is shown in Figure 6, where we plot the electron temperature as a function of geocentric distance in earth radii on a log-log scale. In the region from 2 to $5R_e$ the electron temperature increases from 0.3 eV at $2R_e$ to 1.6 eV at $5R_e$. The accuracy of the IMP temperature measurement is dependent upon the straight line fit through corrected

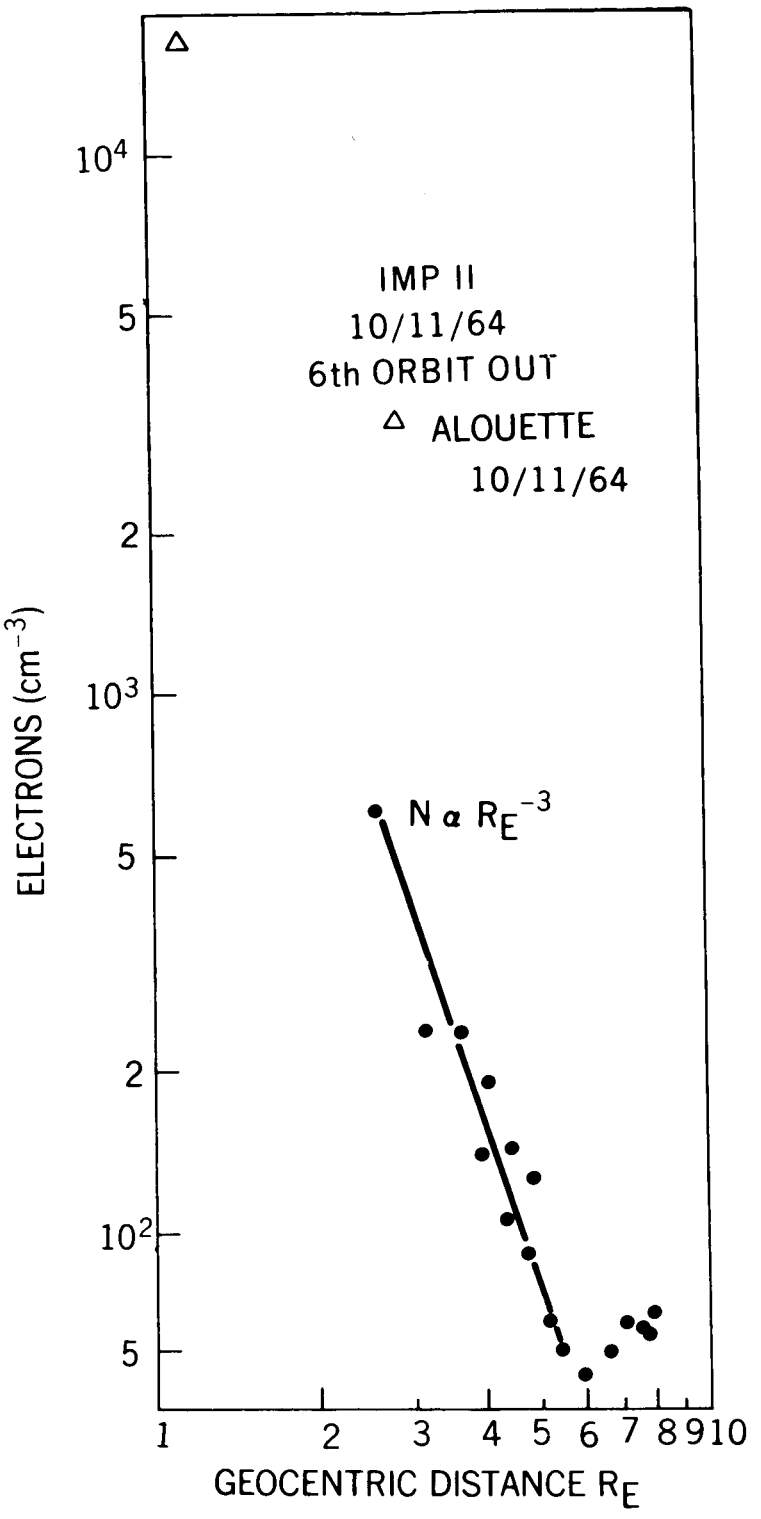

Figure 5. Electron density profile obtained on the 6th outbound orbit of 11 October 1964.

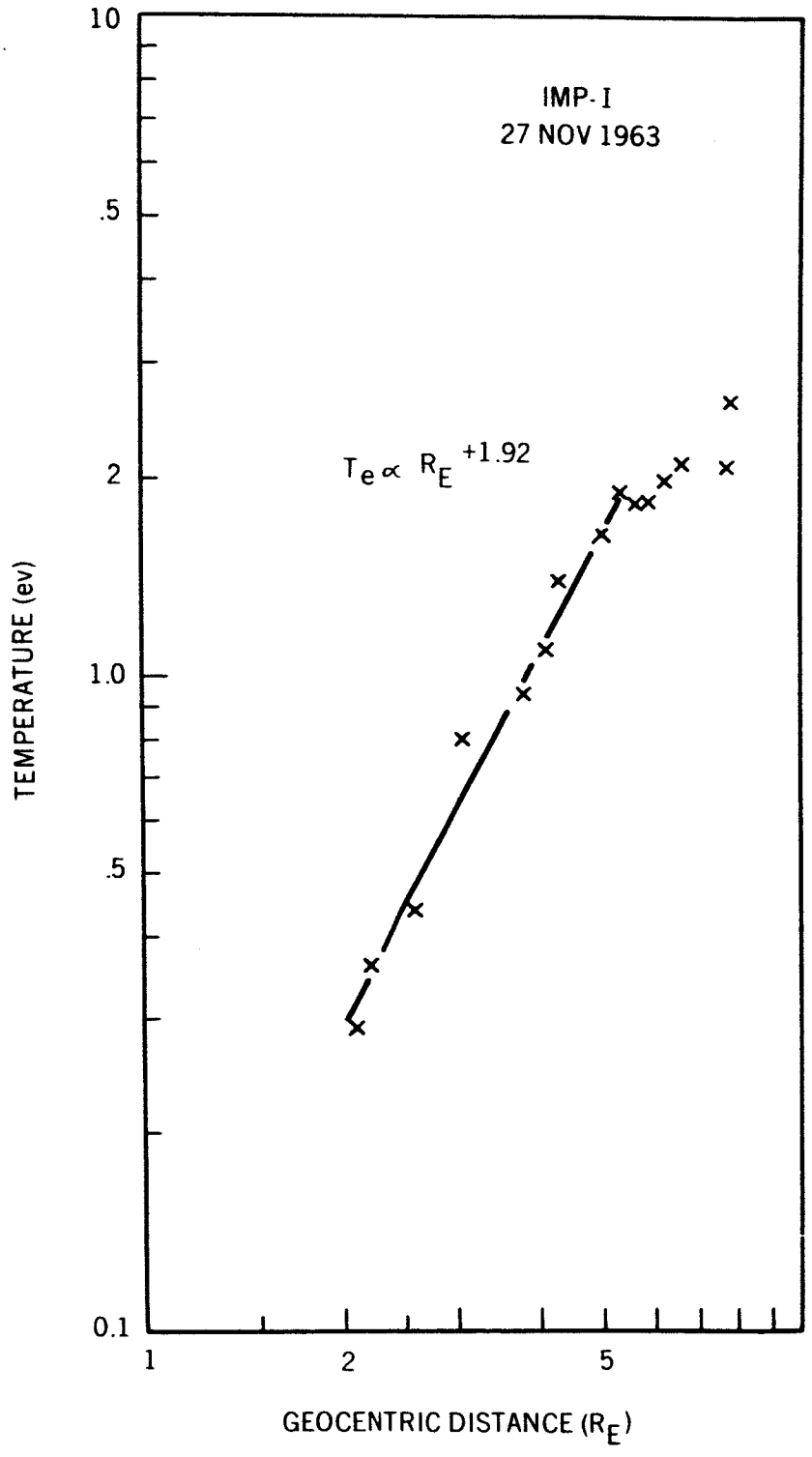

Figure 6. Electron temperature profile as a function of geocentric distance. IMP I data of 27 November 1963.

electron current values, i.e., the solid dots in Figure 2. In general, the fit of these values to a straight line is good over a hundred-to-one range in current amplitude; thus the electron temperature, i.e., the line slope, can be determined to within ±0.1 eV. The data points in the 2 to $5R_e$ region fit rather well to a power law $T_e \alpha R_e^{+1.9}$. The 11 October 1964 profile, Figure 7, is also smoothly increasing with a +1.9 power of the radial distance. At distances from 5 to $10R_e$ the electron temperature remains in the range from 1 to 3 eV. Thus, we see that within the $5R_e$ distance the pressure of the electron gas as derived from these profiles of temperature and density is inversely proportional to the distance; from $5R_e$ to $15.9R_e$ (apogee) the pressure remains approximately constant.

In order to organize the large volume of data obtained from IMP II we have set up criteria whereby the data is separated into two broad categories on the basis of the observed plasma parameters: 1) A "quiet" condition exists when we observe a smooth temperature profile in the region below $5R_e$ accompanied by a high ratio of the thermal electron current to the more energetic electron current. Within the magnetosphere this ratio is generally 10 to 1 or more on the quiet transits; through the magnetosheath the ratio is generally less than 5. Data presented in Figures 4, 5, and 6 is representative of "quiet" conditions. 2) A "disturbed" condition is typified by the fact that the electron temperature reaches values of 1 to 3 eV at distances closer in than $5R_e$, and the high energy component is large so that the ratio of thermal to more energetic electrons is not greater than 5 to 1. Figures 8 through 16 are plots of the temperature and density profiles for nine orbits which have been obtained during quiet transits within a 190° sector of the earth-sun line; the orbit precessed through this 190° sector starting from the sub-solar point at launch. In these profiles the abscissa is in terms of the L parameter. This was done with the hope of studying electron distribution along field lines and to investigate what coupling between the magnetic field and the thermal electrons might become evident.

If we compare the profiles of temperature and density obtained at a sun-earth-satellite angle of 55°, Figure 14, with the profiles taken at an angle of 193°, (Figure 16) we see a remarkable similarity which is not necessarily significant in itself but which points to the fact that on certain days the profiles obtained on the day-side can resemble those obtained on the night-side of earth. As can be seen, all these profiles are approximately uniform in temperature rise and density fall-off, yet no two are identical. Individual transits through the magnetosphere show a factor of 3 variation in density over distances along the orbit of the order of 5000 kilometers. Cole [1964] attributes a changing structure in the magnetosphere plasma to random electrostatic fields which cause irreversible energization and transport of ambient plasma from outer to inner parts of the magnetosphere.

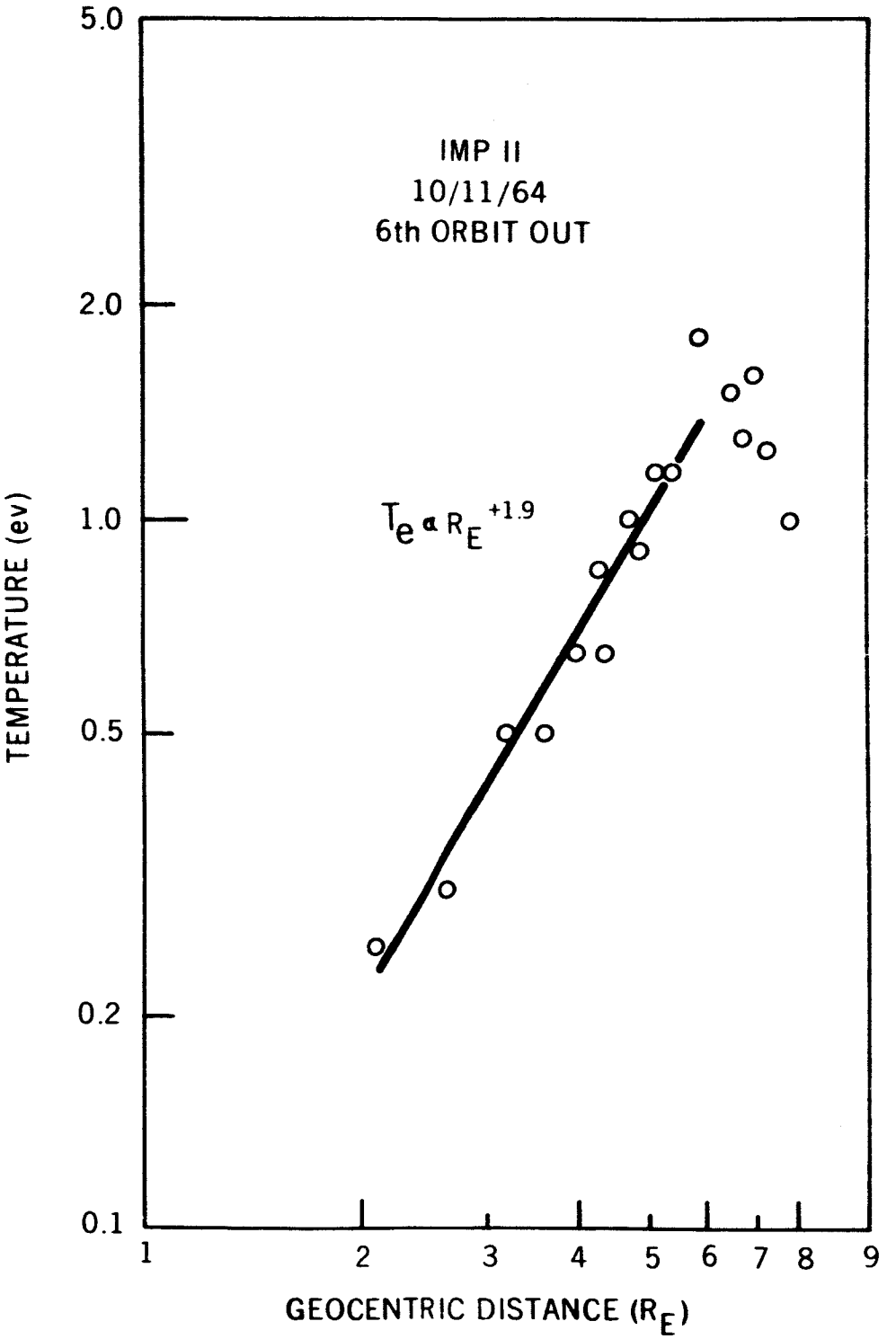

Figure 7. Electron temperature profile obtained on the 6th orbit out, 11 October 1964. This temperature profile was observed simultaneously with the density profile shown in Figure 5.

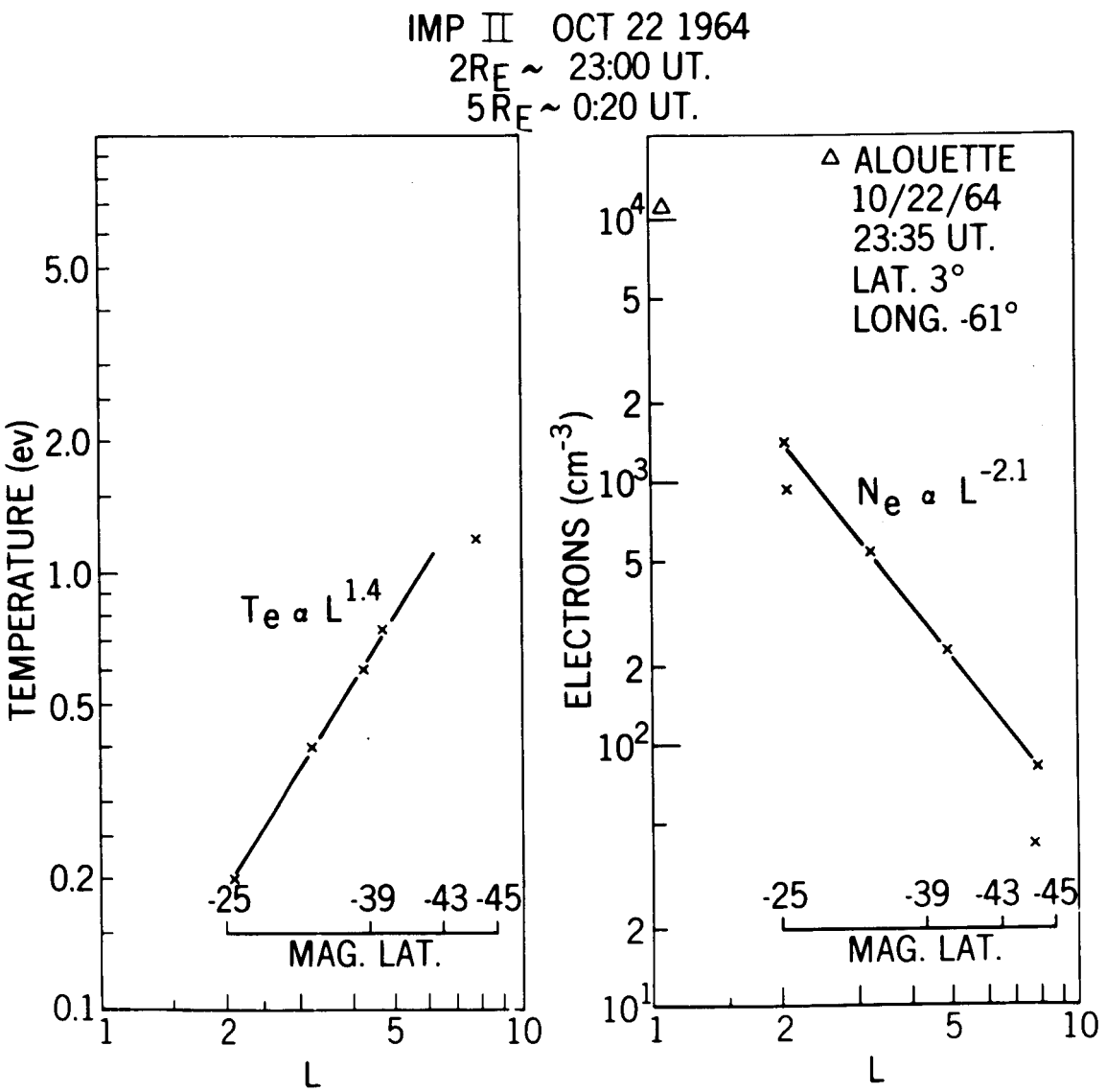

Figure 8. The combined electron temperature and density profiles for 22 October 1964. These observations were made on an outbound trajectory. At the time of the Alouette measurement IMP II was at $3.2 R_e$.

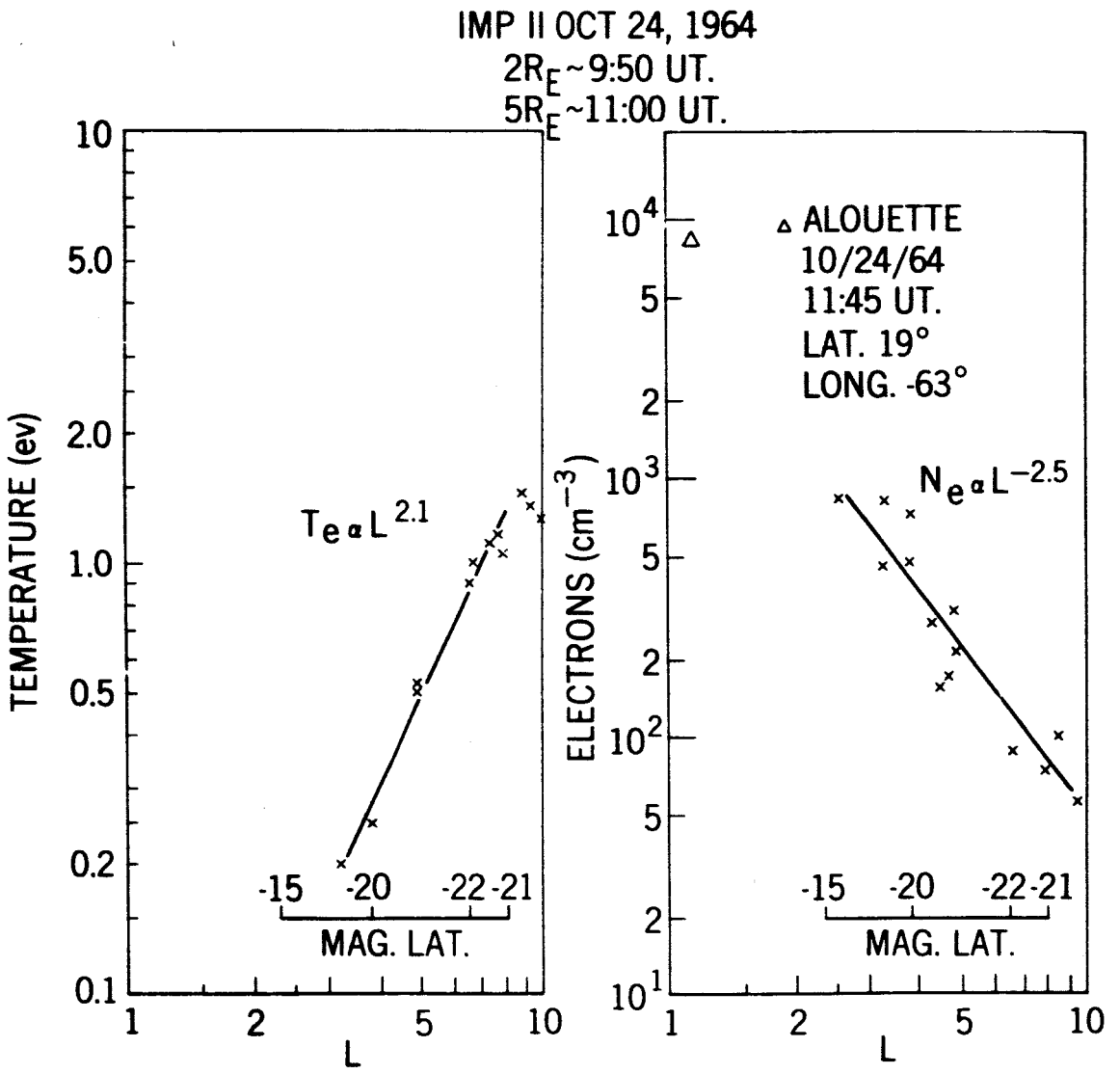

Figure 9. The combined electron temperature and density profiles for the outbound trajectory of 24 October 1964.

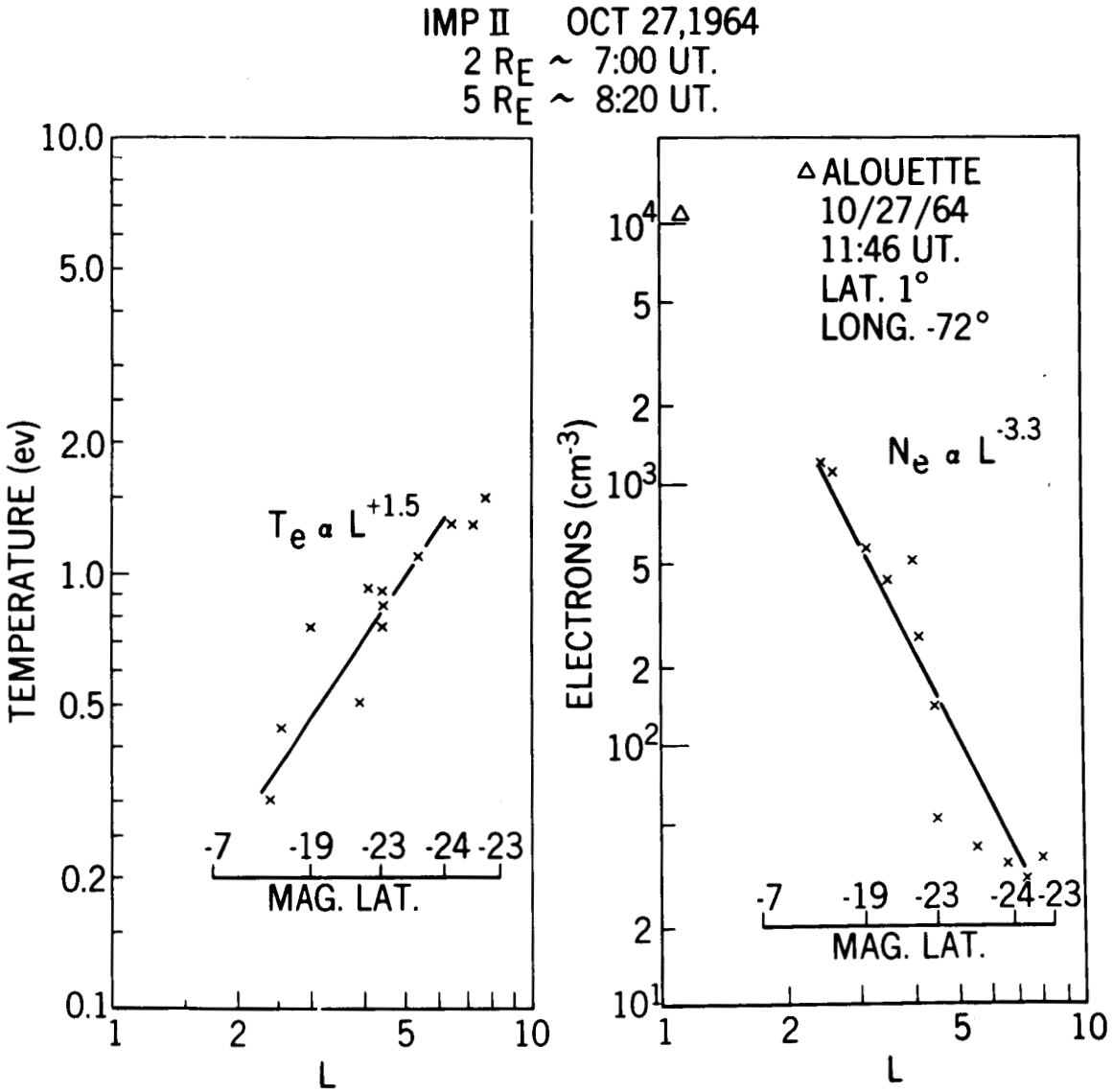

Figure 10. The combined electron temperature and density profiles for the outbound trajectory of 27 October 1964.

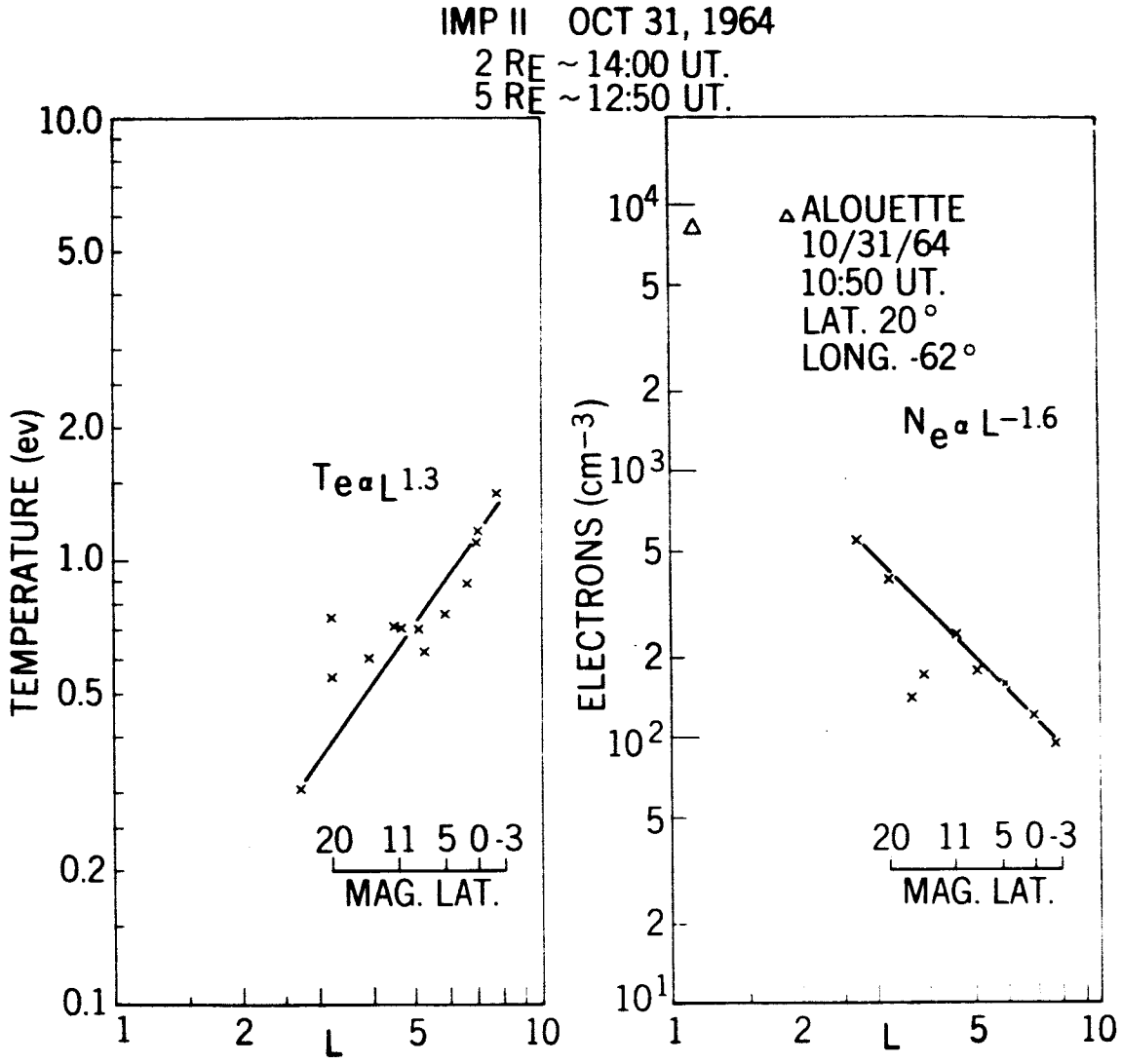

Figure 11. The combined electron temperature and density profiles for the inbound trajectory of 31 October 1964.

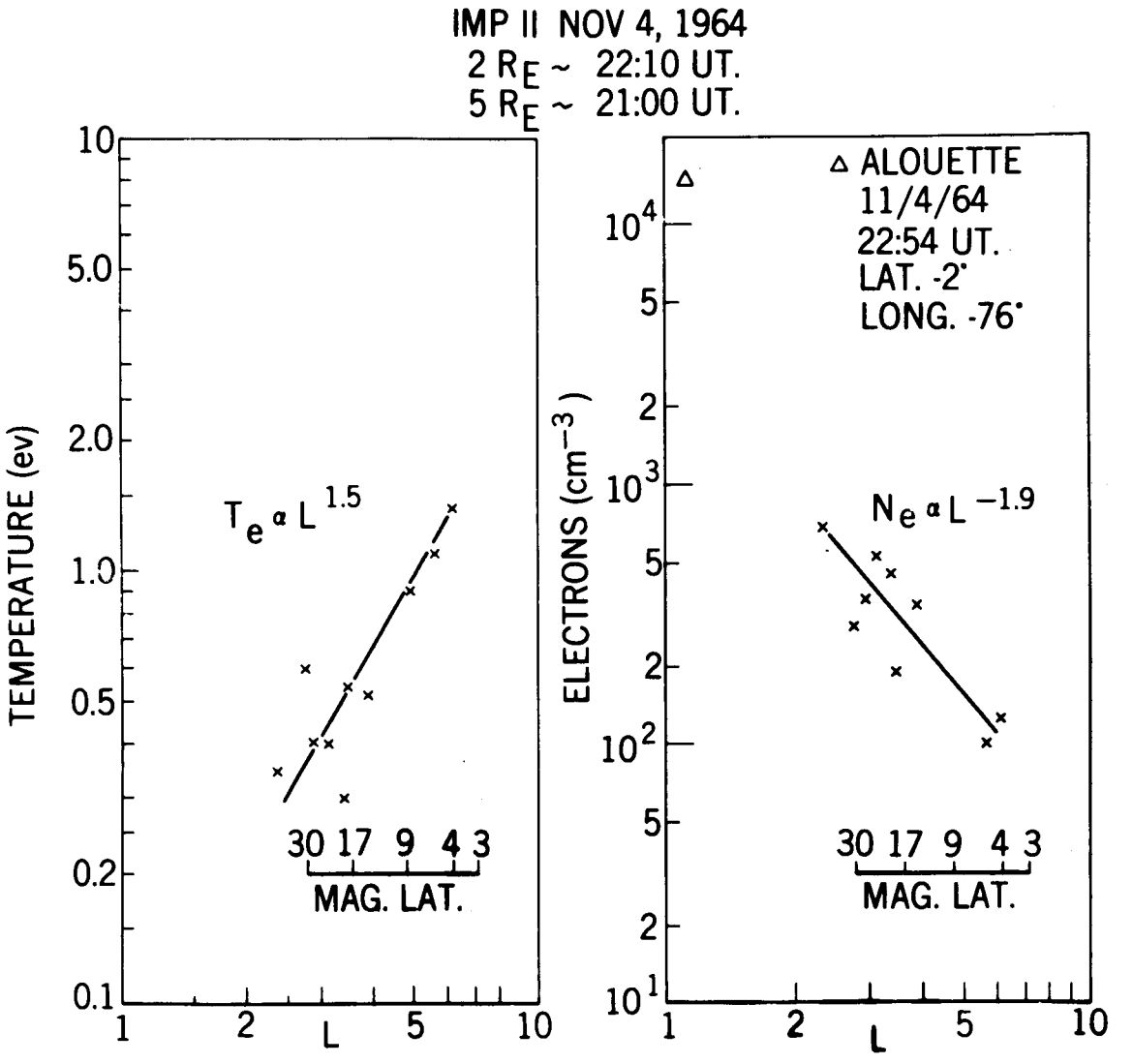

Figure 12. The combined electron temperature and density profiles for the inbound trajectory of 4 November 1964.

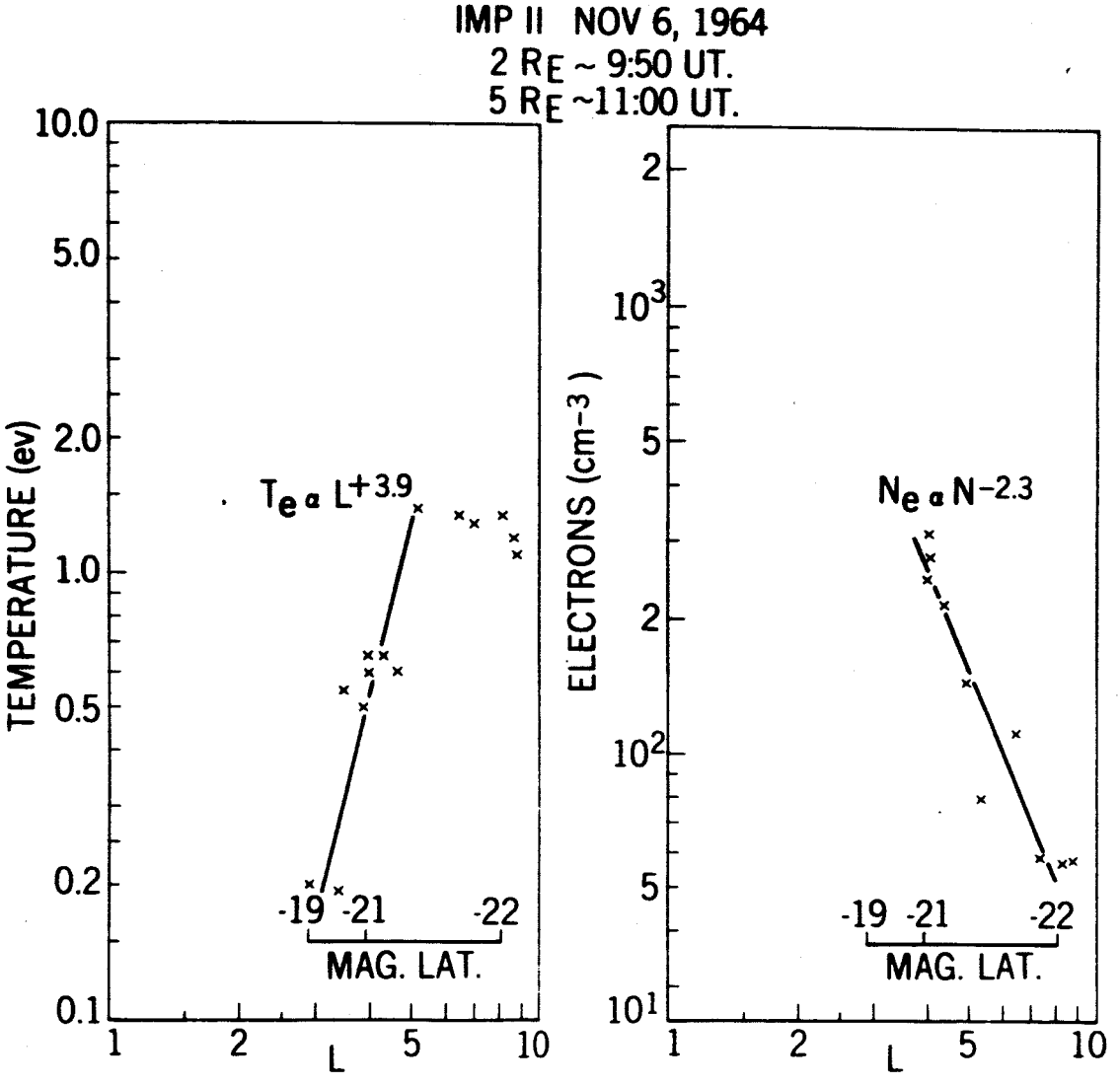

Figure 13. The combined electron temperature and density profiles for the outbound trajectory of 6 November 1964.

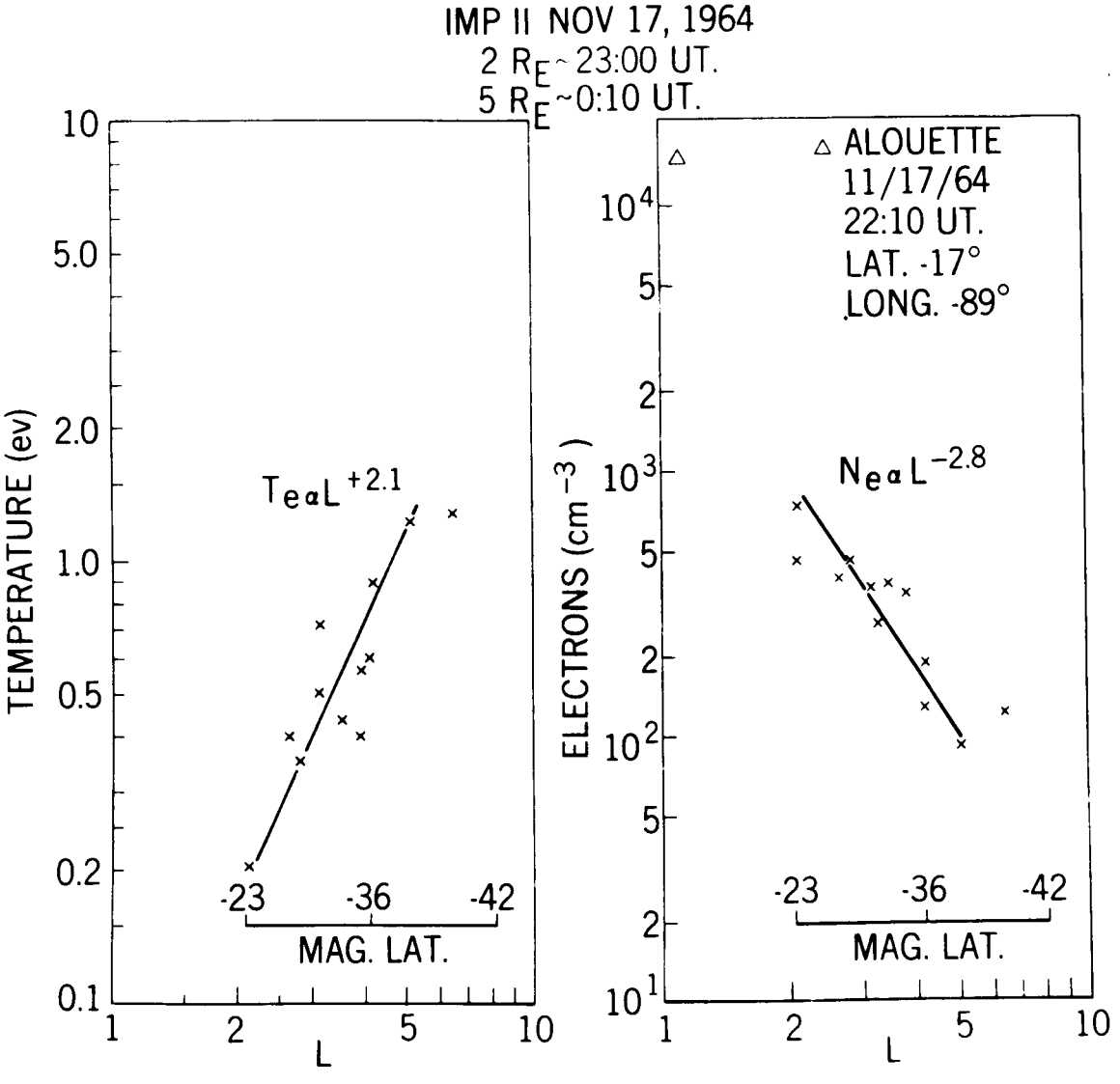

Figure 14. The combined electron temperature and density profiles for the outbound trajectory of 17 November 1964.

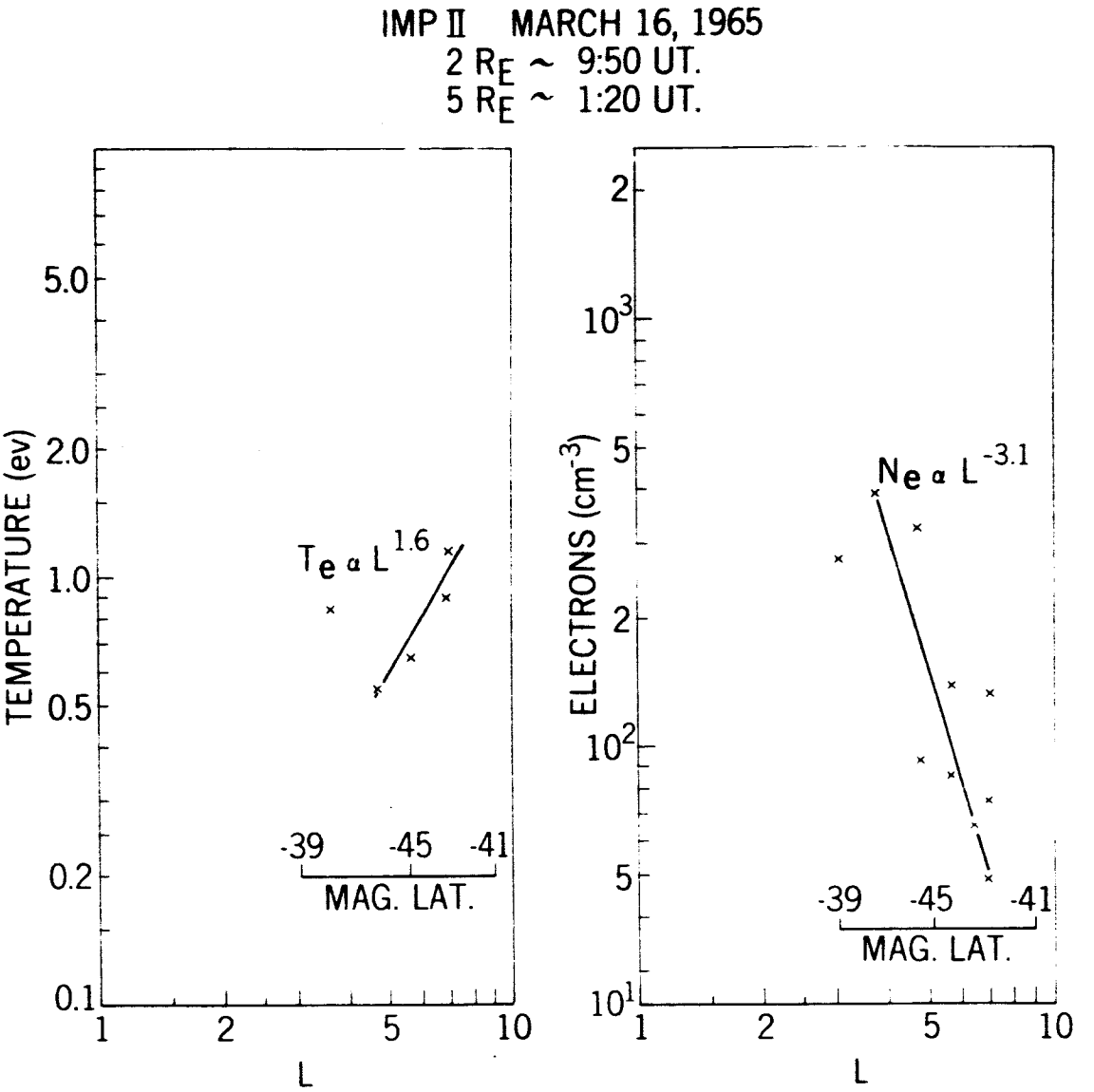

Figure 15. The combined electron temperature and density profiles for the outbound trajectory of 16 March 1965.

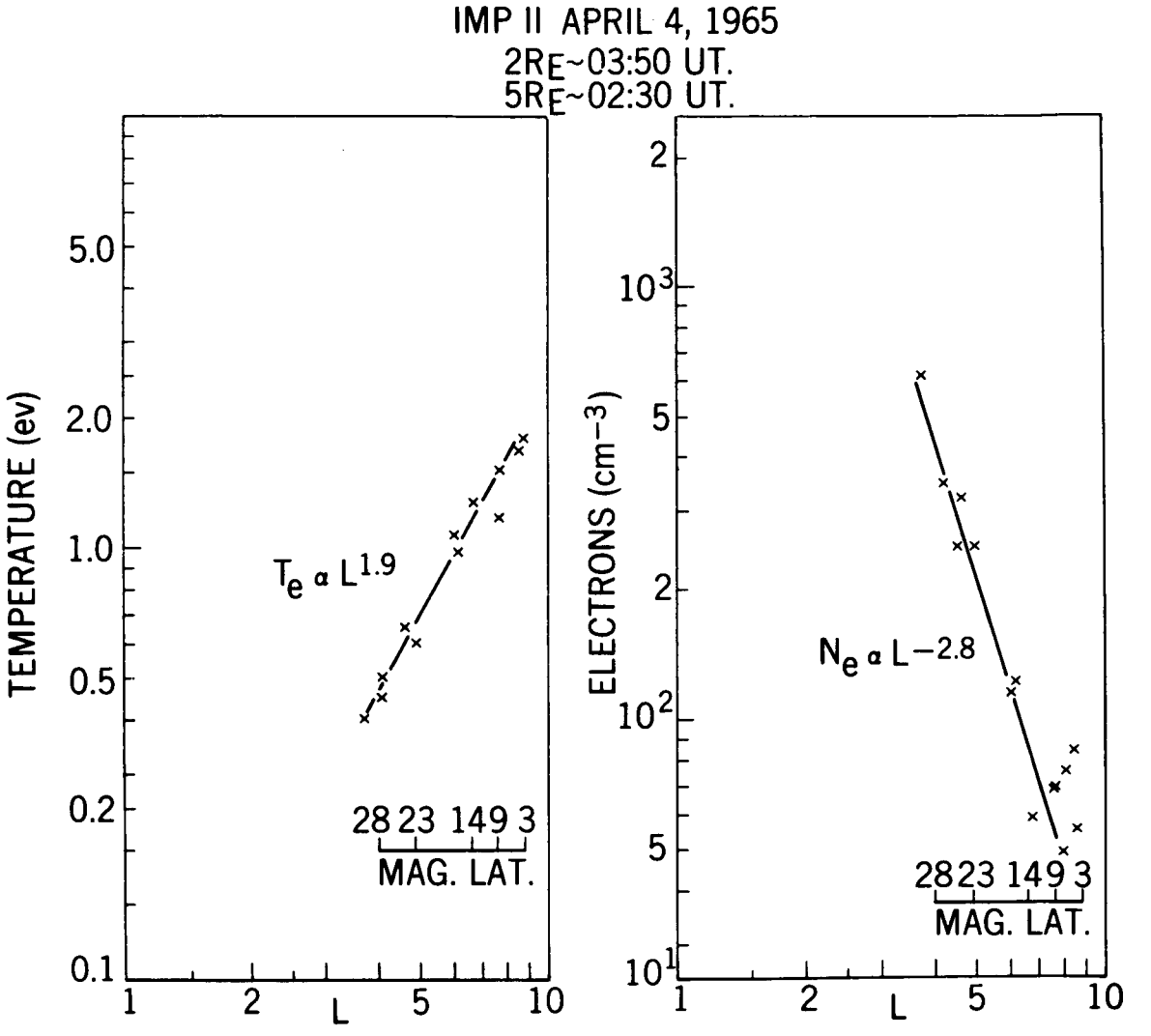

Figure 16. The combined electron temperature and density profiles for the inbound trajectory of 4 April 1965.

The observed electron densities at distances of L equal to 3, 5, and 10, for the time from launch through 5 December 1964 are shown in Figure 17.

These plots represent the observed density over a two month period on the day-side of the earth. The angle between the sun-earth-payload line and the precessing orbit line of apsides is shown at the top of the figure (LSEP).

It is apparent from the figure that the observed density is quite variable when viewed on a two month time scale. The fluctuations of the L=3 curve and the L=5 curve are larger than the fluctuations at L=10. In addition a correlation is evident between the large fluctuations at L=3 and at L=5, whereas neither one of these two curves correlates well with the L=10 curve. The observed fluctuations are deemed to be temporal in nature; no systematic variations are noted as the orbit precessed 70° toward the sunrise terminator.

In an attempt to search for a relationship between the geomagnetic field fluctuation and the magnetospheric plasma, we have computed the correlation coefficient between the 3 hourly average K_p indices (Lincoln, 1965) and the observed electron densities for spacecraft positions on several selected magnetic L shells. The data have been grouped in two classes: 1) Data obtained on days having a magnetic disturbance classified as "moderately severe" and 2) data obtained on other days. For this analysis we have used electron densities obtained during the period October 4 to December 5 on L shells 3, 5, and 10.

To test the effective propagation time relationship between the field fluctuation at the earth's surface and the plasma density at the spacecraft position the cross correlation coefficient was computed between the magnetic indices K_p (T_o) and the density $n(L, T_o - T)$ for time displacements T in the time interval -30 to +30 hours.

Figure 18 shows that for the non-storm days there is no significant correlation between n and K_p for the time shifts which we have considered. We therefore conclude that for the time period of the geomagnetic data which has been used (three hour averages) there is no generally prevalent stable relationship between the K_p index and the magnetospheric thermal electrons.

For the storm days in the time interval considered, the picture is quite different. Figure 19 shows the cross correlation coefficient as a function of time displacement. Most apparent is the significant correlation which is evident for the ±6 hour interval about zero time shift. The magnetic control of the plasma indicated by this correlation is interpreted at this time to reflect the mean duration of the storm rather than the details of the magnetic control. Detailed discussion of the time structure and significance of this preliminary storm correlation will be deferred until more data becomes available.

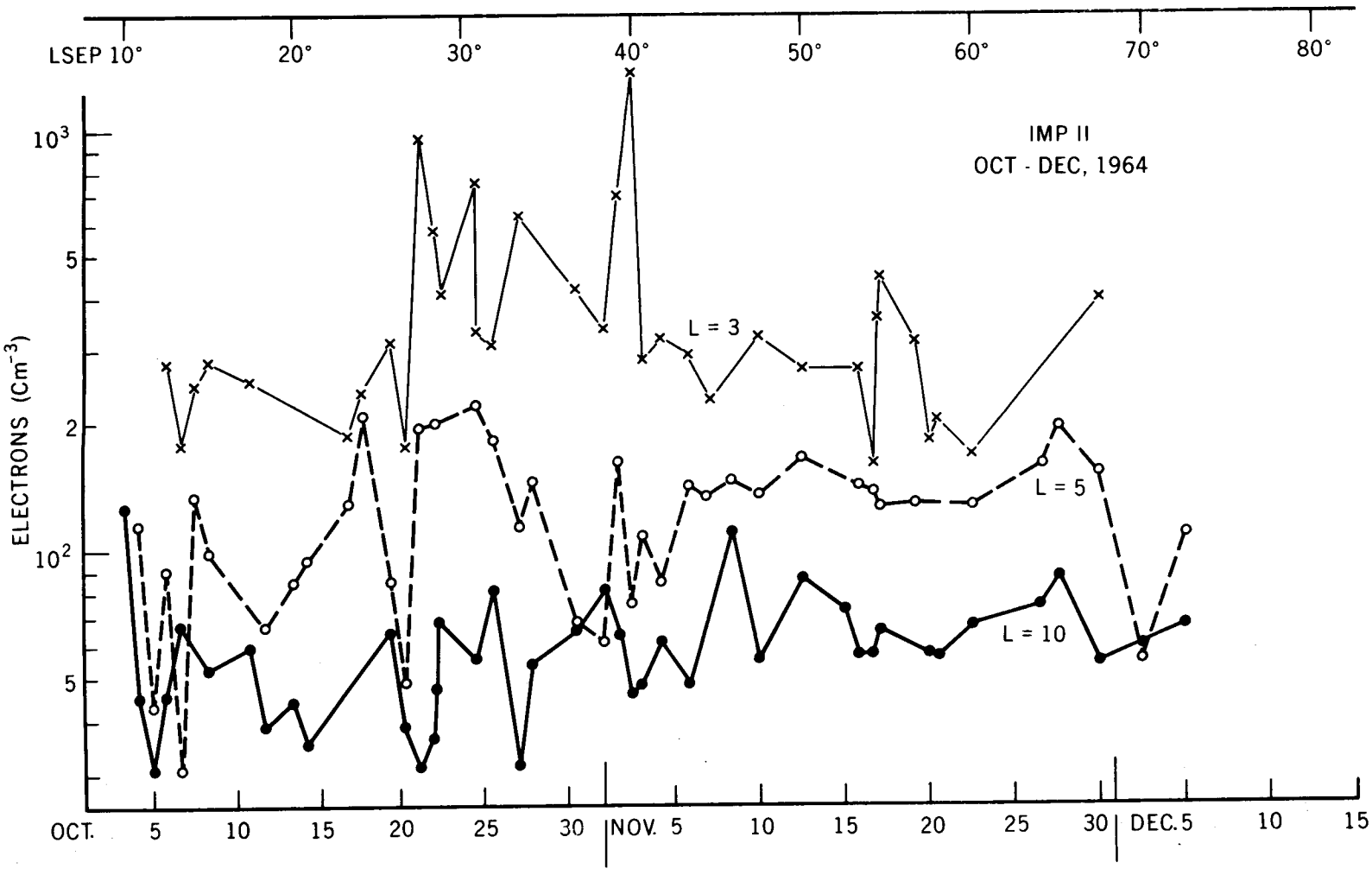

Figure 17. A summary of observed density variations on different L shells as a function of time in orbit.

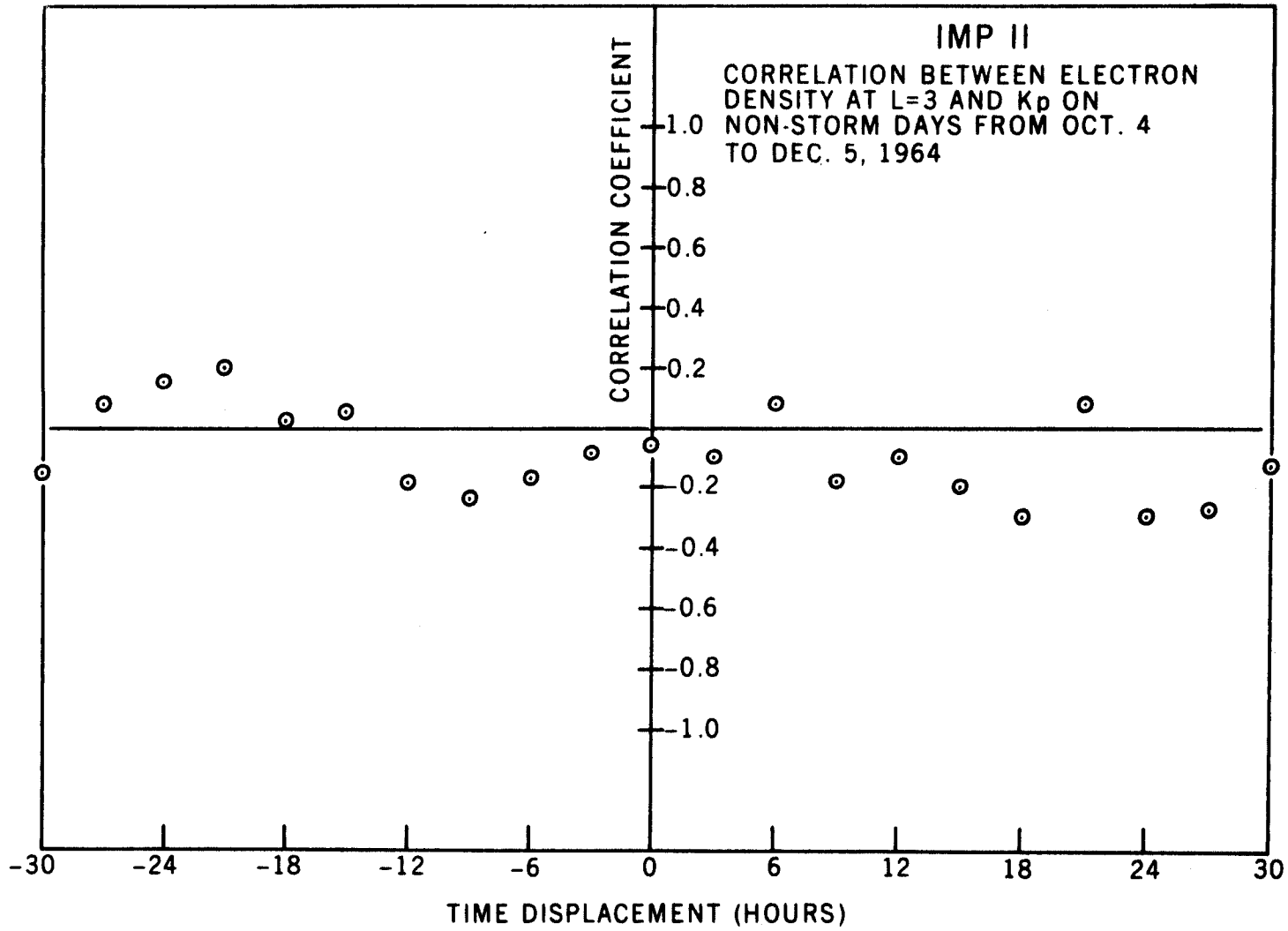

Figure 18. The cross correlation coefficient between electron density and K_p on non-storm days plotted as a function of time displacement between the measurements.

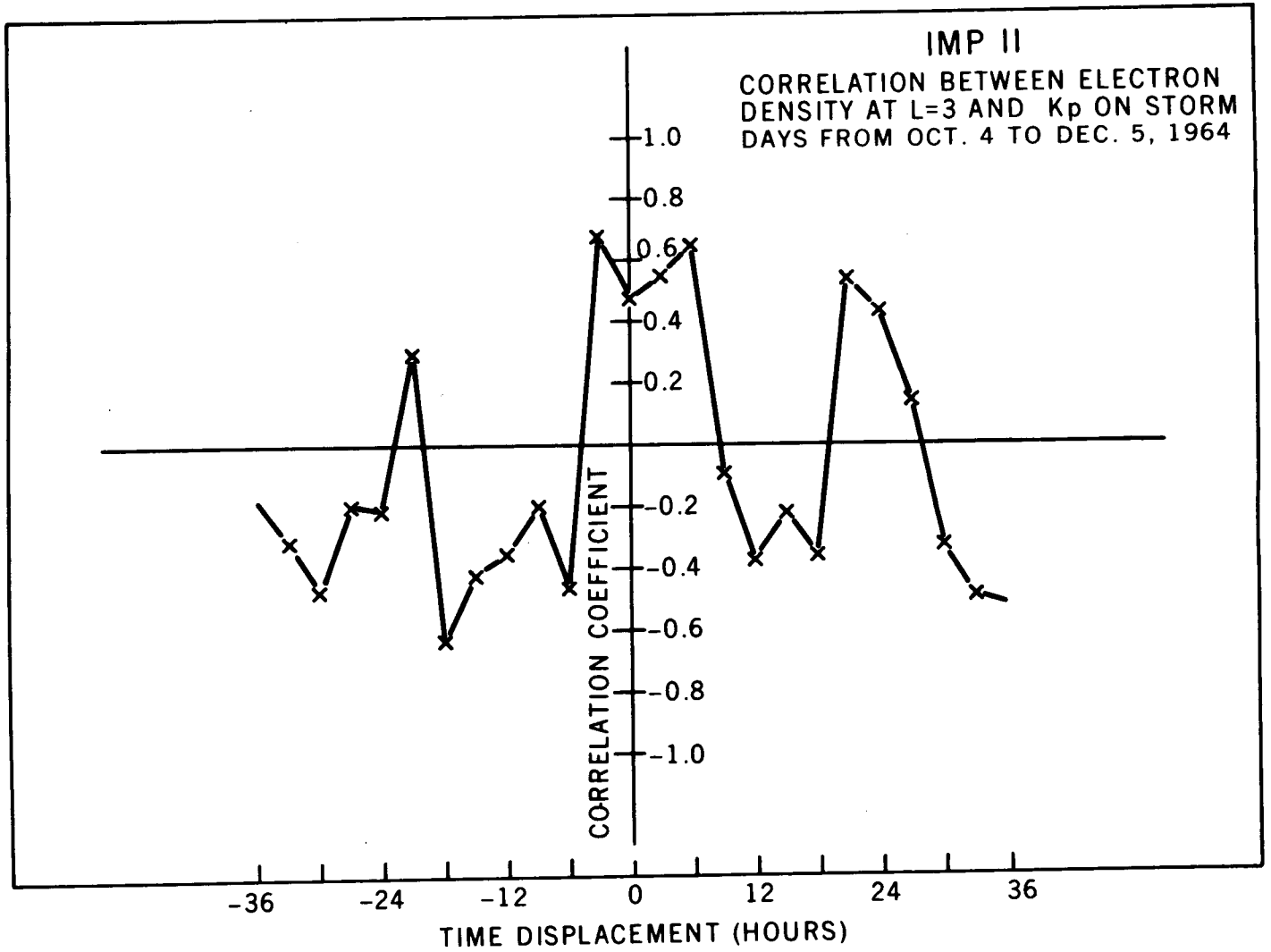

Figure 19. The cross correlation coefficient between electron density and K_p on storm days plotted as a function of time displacement between the measurements.

2. Magnetosheath and Solar Wind Regions

It has been consistently observed that at some point beyond $5R_e$ there is a variable, rapid increase in the energetic component of plasma. A typical example of this is shown in Figure 20 where we have plotted the flux of the energetic residual negative component versus geocentric distance in earth radii. This increase is of the order of a factor of 10 over the energetic component present within the magnetosphere, and its presence constitutes our definition of the magnetosheath boundaries. At the time of this enhancement, there is no significant change in the ambient thermal plasma. The IMP II orbit did not penetrate much beyond the shock front and more detailed discussion of the solar wind region and boundary phenomena is deferred to a later paper in which IMP C results out to $40R_e$ can be included.

Figure 21 is a plot of the observed density at apogee ($15.9R_e$) for the period from 7 October to 5 December 1964. Indicated on the figure is the period of time during which apogee occurred in the solar wind region as indicated from our data; subsequent to 25 October the shock front was apparently not penetrated.

From Figure 3 we see that for each orbit the satellite spends more than 10 hours at distances beyond $15R_e$; thus for the period from launch through 25 October we have accumulated a minimum of 120 hours of data in the solar wind region. During this entire period of observation, the average electron density was $50\,cm^{-3}$. The value of 50 electrons cm^{-3} refers to the density of thermal electrons whose measured temperature lies between 1 and 2 eV.

The density of 1 to 2 eV plasma should be distinguished from measurements by Neugebauer and Snyder [1962]; Bridge, et al., [1964]; and Wolfe, et al., [1965].

In all three of these works, the experiment was not sensitive to the presence of particles whose energy was less than 65 eV.

Electron density measurements in this region have also been obtained from lunar radar reflection observations. Howard et al., [1965] interpreted the Doppler shift measurements at two different frequencies in terms of the total columnar electron content between the earth and the moon. They used simultaneous Faraday rotation and ionospheric sounding measurements to correct their measurement for the ionospheric electron content. Assuming a uniform density in cislunar space, they then obtain 30 +70/-150 and 100 +70/-150 cm^{-3} as the average electron densities 35° and 45° from the noon meridian in good agreement with the present results.

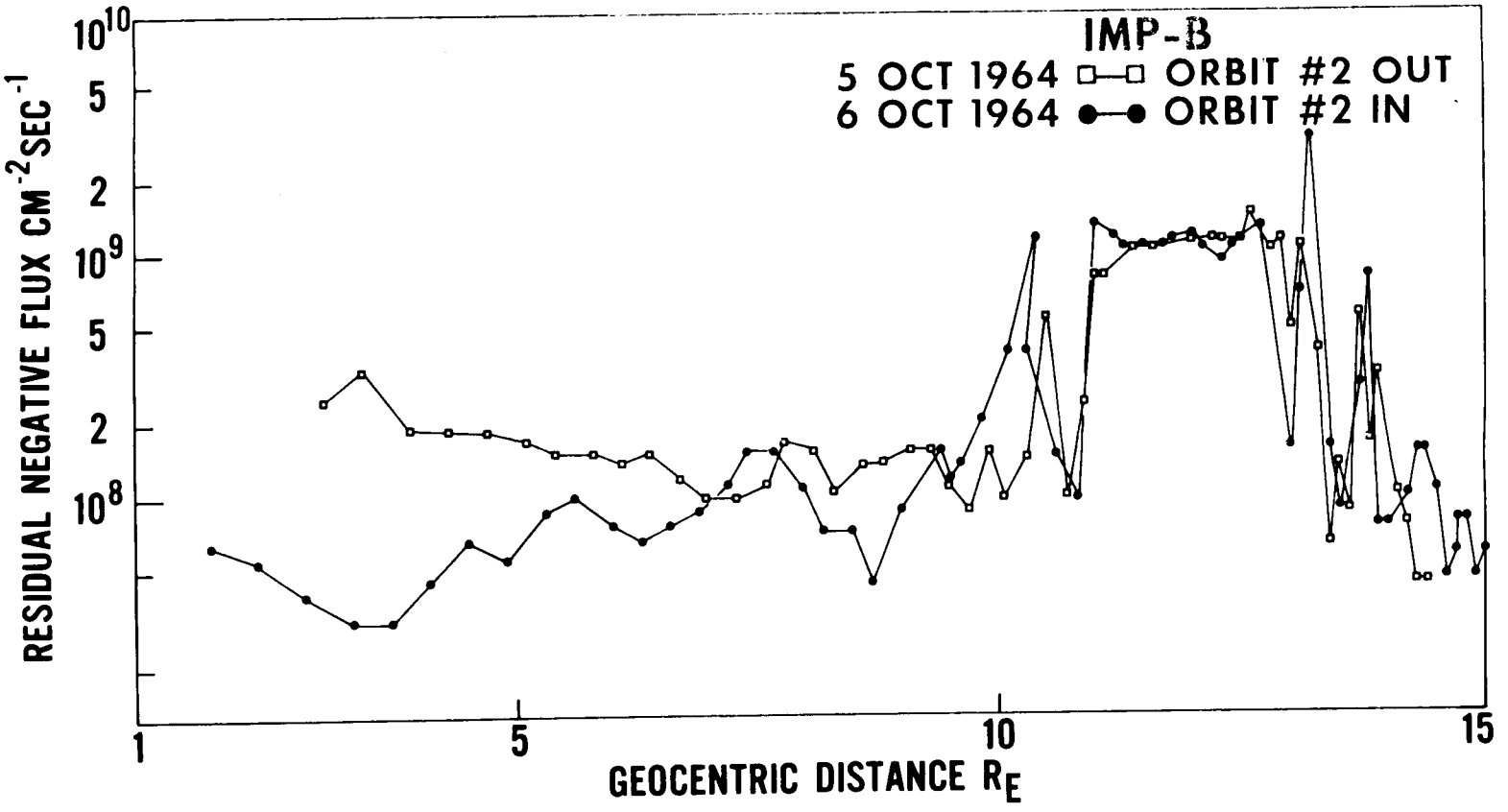

Figure 20. Plot of the residual negative current flux, observed during the second orbit, as a function of geocentric distance.

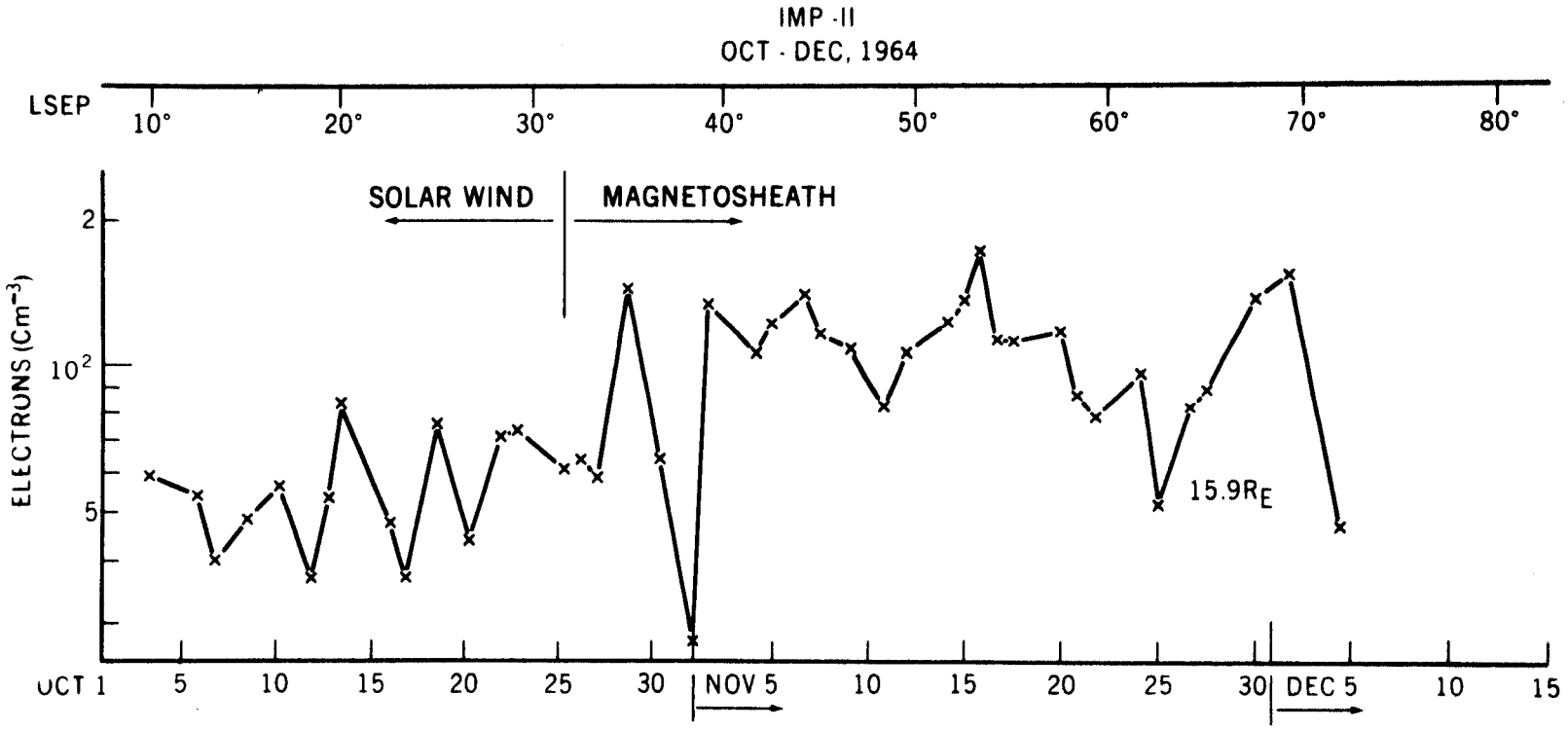

Figure 21. A summary of observed density variations at apogee (15.9R_e geocentric) as a function of time in orbit.

To verify the existence of charge neutrality and to exclude the possibility of a significant number of photoelectrons within the spacecraft sheath, we have examined typical ion retardation curves. Figure 22 represents a group of data obtained at $14.0R_e$. At this distance the current to the ion trap is governed solely by diffusion since the satellite velocity is approximately 10^5 cm/sec, whereas the velocity of a 2 eV proton is approximately 2×10^6 cm/sec. From these data we compute, using the geometric area of the aperture A_G, an ion density of 300 ± 50 protons cm^{-3} at a temperature of 2 eV. The electron density measured at this distance is $350 \pm 40\, cm^{-3}$. From these measurements we conclude that an upper limit for the sum of local photoelectron density and local deviation from strict charge neutrality is $(50 \pm 65)\, cm^{-3}$.

Wolfe et al. [65] reports that the solar wind proton density of particles whose velocity is of the order of 500 km/sec rarely exceeds $3\, cm^{-3}$. Bridge et al. [1964] reports a solar wind proton flux of 10^8 to $10^9\, cm^{-2}\, sec^{-1}$ and a wind velocity of 250 to 440 km/sec. Both of these measurements yield an energy density of the order of 2 to 20×10^{-9} ergs cm^{-3}. The energy density of a 2 eV plasma of density 50 electron-ion pairs per cm^3 is 3×10^{-10} ergs/cm^{-3} which is the magnetic energy density of a 9 gamma field.

3. Summary of Results

Figure 23 is a summary of our observations of thermal electrons in the dayside magnetosphere during selected "quiet" transits. Shown is a projection onto the ecliptic plane of those traverses during which we observed a uniform increase in temperature with distance and at the same time observed that the ratio of "thermal" to "energetic" current components was at least 10 to 1 within the magnetosphere. The shapes of the indicated shock and magnetopause were taken from Ness [1964]. Magnetosheath data, indicated by the solid lines in the figure for each day of transit, are characterized by having the ratio of the two currents change abruptly from 10 to 1 to a ratio of 5 to 1 or less. The shock front was then located as a best fit to the data.

The dashed curves in the figure indicate isotherms that can be drawn through the data points, open circles, for each "quiet" transit. Beyond $5R_e$ the thermal electron temperature remains essentially constant even as we cross the magnetopause. The largest temperature value occurs at the inside of the indicated shock front. Beyond the shock front the temperature drops to 1.2 eV. Thermal electrons do not appear to undergo any marked changes in temperature or density across the magnetopause. This generalized picture is supported by all the data of Figures 8 through 16, as well as the plots of Figures 23 and 24. In Figure 24 we have plotted the data characterized as "disturbed;" as can be seen isotherms cannot be drawn through the indicated temperatures values. Electron

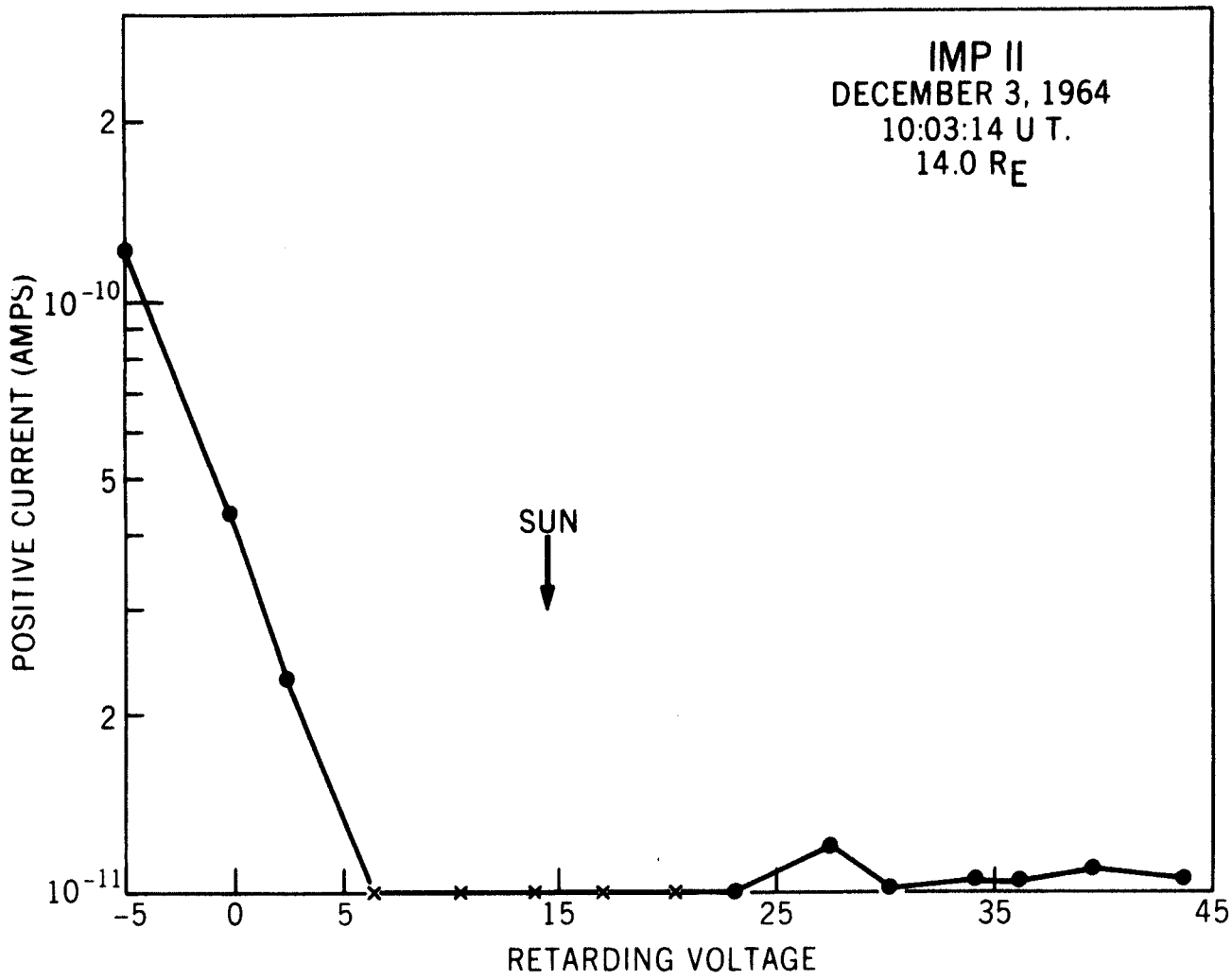

Figure 22. Sample ion current-voltage retardation curve, the logarithmic positive current is plotted as a function of the linear retardation potential in volts. The five data points symmetric about the sun arrow (crosses) indicate that the electrometer is being driven below zero volts by a negative current component due to photoemission currents from the suppressor grid.

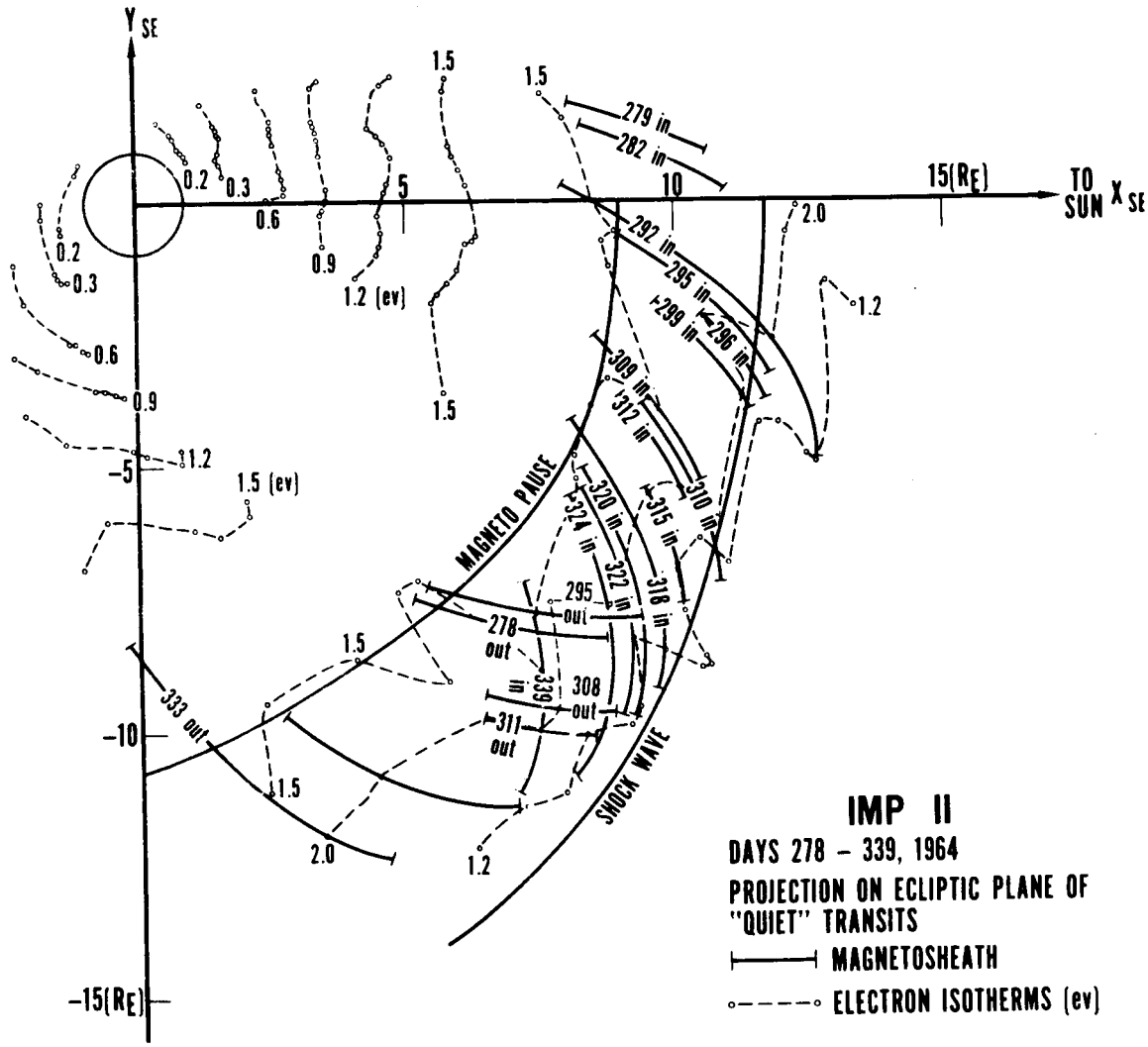

Figure 23. Projection on ecliptic plane of "quiet" transits, electron temperature data, and enhanced levels of high energy electron current component, as a function of days in orbit.

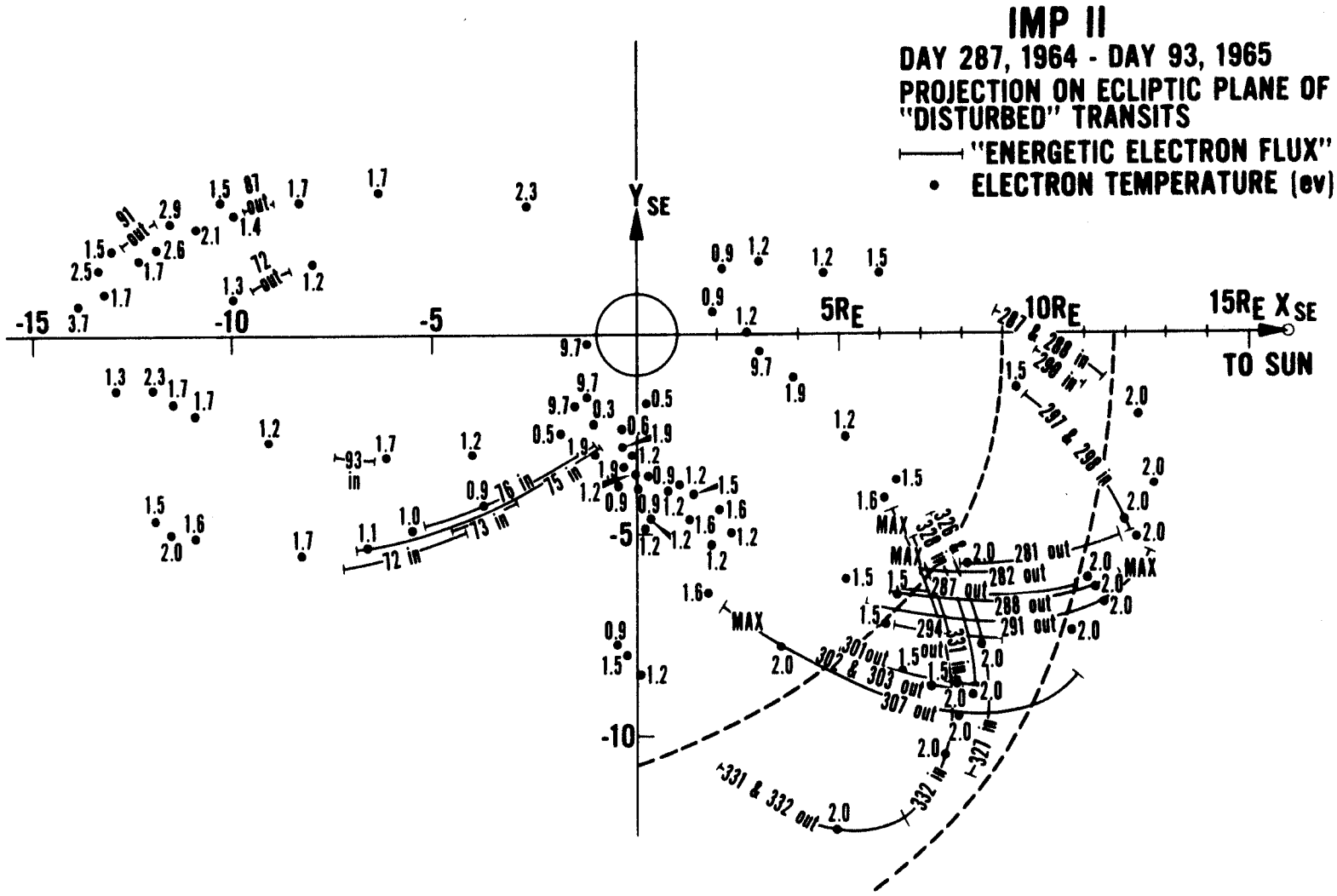

Figure 24. Projection on ecliptic plane of "disturbed" transits, electron temperature data, and enhanced levels of high energy electron current component, as a function of days in orbit.

temperatures are generally in the range from 1 to 2 eV; the difference between the two conditions is that "quiet" transits have a more ordered temperature structure. In Figure 24 we observe what seems to be a maximum temperature of 2 eV which occurs with some consistency near the indicated shock front. On the dark side of the earth the temperature ranges primarily between 1.2 eV and 2.5 eV; only isolated instances of temperatures lower than 1.0 eV or higher than 2.5 eV have been observed. The appearance of regions of enhanced high energy electron current components does not correlate with the thermal or low energy temperature values. The appearance of the high energy component current is reminiscent of Anderson's [1965] observation of enhanced islands of 40 keV electrons as seen on the dark side with IMP I.

V. CONCLUSIONS

The integral spectrum for low energy electrons has been measured with detailed definition of temperature and number density throughout the IMP II orbit. Electrons are found to have a Maxwellian distribution at energies below 2.0 eV. The electron temperature is found to increase by about a factor of ten within the distance from 2 to 5 earth radii; the increase is generally as the square of the radial distance. In this same region the electron density decreases as the inverse cube of the distance; thus the pressure of the thermal electron gas is falling off approximately inversely proportional to the distance. From $5R_e$ to $16R_e$ this pressure remains constant. A preliminary check of ion current measurements indicates that ion densities and temperature are in agreement with the electron measurements reported on here. During magnetically disturbed days a statistically significant correlation is found to exist between the measured electron density variation at L-shells below 5, and the K_p magnetic index. On all other days the correlation is not statistically significant.

The location of the magnetopause is not evident in the low energy electrons; the thermal electron density and the temperature remain constant across the magnetopause. An intensity increase is noted in the energetic electron component in the magnetosheath; the boundaries of the magnetosheath can be determined with some consistency on this basis. The density of thermal electrons, $50\,cm^{-3}$, has been measured at $15.9R_e$ which is presumably in the solar wind region.

REFERENCES

Anderson, K. A., Energetic electron fluxes in the tail geomagnetic field, J. Geophys. Res., 70, 4741-4763, 1965.

Angerami, J. J. and D. L. Carpenter, Whistler studies of the plasmapause in the magnetosphere-2, J. Geophys. Res., 71, 711-725, 1966.

Bridge, H., A. Egidi, A. Lazarus, E. Lyon and L. Jacobson, Preliminary results of plasma measurements on IMP-A, Proceeding of the Fifth International Space Science Symposium, Florence, May 8-20, 1964, pp. 969-978. North-Holland Publishing Company, Amsterdam, 1965.

Carpenter, D. L., Whistler evidence of a 'Knee' in the magnetospheric ionization density profile, J. Geophys. Res., 68, 1675-1682, 1963.

Carpenter, D. L. and R. L. Smith, Whistler measurements of electron density in the magnetosphere, Review of Geophysics, Vol. 2, No. 3, 415-441, 1964.

Carpenter, D. L., Whistler studies of the plasmapause in the magnetosphere-1; Temporal variations in the position of the Knee and some evidence on plasma motions near the Knee, J. Geophys. Res., 71, 693-709, 1966.

Cole, K. D., On the depletion of ionization in the outer magnetosphere during magnetic disturbances, J. Geophys. Res., Vol. 69, 3595-3601, 1964.

Howard, H. T., V. R. Eshleman, G. H. Barry and R. B. Fenwich, Radar measurements of the total cislunar electron content, J. Geophys. Res., Vol. 70, 4357-4363, 1965.

Lincoln, J. Virginia, Geomagnetic and solar data, J. Geophys. Research, Vol. 70, pages 1229, 1751 and 2234, 1965.

Ness, N. F., C. S. Scearce and J. B. Seek, Initial results of the IMP I magnetic field experiment, J. Geophys. Res. 69, 3531-3570, 1964.

Neugebauer, M. and C. W. Snyder, The mission of Mariner 2, preliminary observations, Science, 138, 1095-1096, 1962.

Obayashi, T., Ionospheric experiment using the orbiting geophysical observatory (OGO-A) at the Ionosphere Research Laboratory, Kyoto University, Report of Ionosphere and Space Research in Japan, Vol. 19, No. 2, 214-224, 1965.

Parker, L. W., A computer program for calculating the charge distribution about a space vehicle, Paper presented at American Astronautical Society, 2nd Symposium on Interaction of Space Vehicles with an Ionized Atmosphere, Miami Beach, Florida, November 1965.

Serbu, G. P., Results from the IMP I retarding potential analyzer, Proceedings of the Fifth International Space Science Symposium, Florence, May 8-20, 1964, pp. 564-574. North-Holland Publishing Company, Amsterdam, 1965.

Slish, V. I., The measurement of cosmic radio emission at the frequencies 210 and 2200 kc/s at distances up to 8 earth radii, from the Automatic Interplanetary Station Zond-2, Cosmic Research, Tome III, 760-767, 1965.

Taylor, H. A., Jr., H. C. Brinton and C. R. Smith, Positive ion composition in the magnetoionosphere obtained from the OGO-A satellite, J. Geophys. Res., 70, 5769-5781, 1965.

Wolfe, J. H., R. W. Silva, M. A. Myers, Observations of the solar wind during the flight of IMP-I, submitted to the Journal of Geophysical Research, 1965.